

FIRST PRINCIPLES MOLECULAR DYNAMICS INVOLVING EXCITED STATES AND NONADIABATIC TRANSITIONS

NIKOS L. DOLTSINIS* and DOMINIK MARX†

Lehrstuhl für Theoretische Chemie, Ruhr-Universität Bochum, 44780 Bochum, Germany

URL: <http://www.theochem.ruhr-uni-bochum.de/>

**nikos.doltsinis@theochem.ruhr-uni-bochum.de*

†dominik.marx@theochem.ruhr-uni-bochum.de

Received 9 May 2002

Accepted 16 June 2002

Extensions of traditional molecular dynamics to excited electronic states and non-Born–Oppenheimer dynamics are reviewed focusing on applicability to chemical reactions of large molecules, possibly in condensed phases. The latter imposes restrictions on both the level of accuracy of the underlying electronic structure theory and the treatment of nonadiabaticity. This review, therefore, exclusively deals with *ab initio* “on the fly” molecular dynamics methods. For the same reason, mainly mixed quantum-classical approaches to nonadiabatic dynamics are considered.

Keywords: *Ab initio* molecular dynamics; excited states; nonadiabatic effects.

1. Why do Excited State Molecular Dynamics?

Traditional molecular dynamics simulations rely on a few simple but crucial assumptions. Among the most important ones is the treatment of the atomic nuclei as classical point particles that evolve adiabatically in a single electronic state, which is often taken to be the ground state. In addition, the interaction potential has to be known prior to the simulation in order to be able to evaluate the nuclear forces at each step of the numerical propagation. Within the associated approximations such simulations are a well established and powerful tool for investigating the structure and dynamics of many-body systems — mostly in the framework of condensed matter physics and chemistry. The broadness, diversity, and high level of sophistication of this technique is documented in several excellent monographs, reviews, proceedings, and lecture notes.^{1–9}

One of the most powerful extensions of traditional molecular dynamics has been achieved by

circumventing the need to know in advance the interatomic interaction potentials. Such techniques are now widely known as the “Car–Parrinello scheme”¹⁰ or “on the fly propagation”; other notions such as “*ab initio*”, “first principles”, or “direct molecular dynamics” are also in use.¹¹ It is interesting to note that the 1985 paper by Car and Parrinello¹⁰ is the very last one in the concluding section “Trends and Prospects” in the 1987 reprint collection of “key papers” from the field of atomistic computer simulations.² Moreover, since 1997 the *Physics and Astronomy Classification Scheme*¹² (PACS) includes the special classification number 71.15.Pd “Electronic Structure: Molecular dynamics calculations (Car–Parrinello) and other numerical simulations” in order to classify such techniques.

The basic idea underlying any first principles molecular dynamics method is to compute the forces acting on the nuclei from electronic structure calculations that are performed “on the fly” as the molecular dynamics trajectory is generated. In this

way, the electronic variables are not integrated out beforehand, but are considered as active degrees of freedom. A fair number of review articles dealing with *ab initio* molecular dynamics have appeared over the past decade^{11,13–23} and the interested reader is referred to them for various complementary viewpoints. In the mid-1990s, the original *ab initio* molecular dynamics scheme was extended by lifting the approximation of using classical nuclei. The resulting so-called *ab initio* path integral technique^{24–27} is a combination of *ab initio* molecular dynamics¹⁰ and path integral molecular dynamics.^{28–30} Similar to traditional molecular dynamics, it was assumed in first principles molecular dynamics that the adiabatic time evolution of the electronic degrees of freedom takes place in the instantaneous ground state.

The present review article focuses on approaches that cross this remaining frontier, i.e. it deals with molecular dynamics simulations beyond the Born–Oppenheimer approximation. This requires that not only the electronic ground state is treated, but, in addition, at least one excited state. Furthermore, the focus of this review is on *dynamical* simulation techniques that allow to analyse the time evolution of *molecular* systems with *many* coupled degrees of freedom possibly in *condensed phases*³¹ such as liquids, solids, glasses, or biomatrices.³² In addition, chemical reactions, i.e. the breaking and making of covalent bonds should be accessible with these methods. Generic problems in this class are strongly excited liquids or solids (induced by laser irradiation or extreme temperatures), photoinduced reactions of impurities or molecules that are solvated in liquids or embedded in solids, or phenomena such as excited-state proton transfer occurring in solvated molecules in the gas or liquid phases. The development of nonadiabatic *ab initio* molecular dynamics methods is further motivated by organic photochemistry³³ and the recent experimental advances in ultrafast photochemistry.^{34,35} Many photochemical processes take place on a femtosecond time scale driven by conical intersections or avoided crossings^{33,36–38} of different potential energy surfaces causing the Born–Oppenheimer approximation to break down.

All these requirements preclude from the outset methods that rely crucially on an *a priori* parameterization of the interatomic interactions (leading either to a global “potential energy surface” or to a “force

field” composed of few-body interactions such as pair potentials). An appealing solution is the Diatomics-in-Molecules (DIM)^{39–51} method which cheaply provides electronic eigenvalues and atomic forces for a multitude of molecular valence states. However, although the DIM method works remarkably well for some simple systems such as cationic rare-gas clusters^{52–55} and isoelectronic systems^{56–59} it is not generally applicable to more complex systems. In order to maximize the range of applicability, excited state molecular dynamics methods must therefore be based on “on the fly” electronic structure calculations. Furthermore, typical molecular dynamics runs have to include at least of the order of 10,000 to 100,000 time steps to allow for a meaningful statistics or reasonable correlations in time to be analyzed. This implies that of the order of 10,000 to 100,000 electronic structure calculations have to be performed in order to produce a single useful trajectory! Bearing this in mind, it is clear that computationally demanding (“expensive”), highest-accuracy methods cannot be employed beyond a few interacting electrons. Thus, quantum-chemical approaches that take into account electron correlation (such as, for instance, many-body perturbation theory, configuration interaction, or coupled cluster theories) are currently at the borderline of being useful within the present context. However, it should be kept in mind that this might change in the near future due to advances in (approximate) linear-scaling methods⁶⁰ also for such correlated methods.^{61–63} An alternative might be the vast field of semiempirical methods (see for instance⁶⁴), but there the problem is that they often appear less general, flexible or suited to describe chemical reactions. However, such methods have been a useful tool for optimizations of conical intersections.⁶⁵ Since this review focuses on methods where the entire system is treated on an equal footing, the so-called quantum-classical hybrid methods (now often abbreviated as “QM/MM” methods) will not be covered, although impressive progress has been achieved in recent years in treating local excitations. A MM-VB approach, for example, has been applied with great success to study organic photochemistry.^{66,67} Hybrid *ab initio*/interpolation schemes have been proposed recently^{68,69} in an attempt to reduce the computational demand of first principles molecular dynamics simulations. A

valuable alternative to these traditional quantum chemistry methods is presented by density functional theory^{70,71} as based on the papers by Hohenberg, Kohn, and Sham.^{72,73} It is appealing since the cost/performance ratio is favorable. Furthermore, there is a continued effort to describe also excited electronic states within this approach and generalizations thereof. The main part of this overview will concentrate on such methods excluding, however, sophisticated techniques such as the GW or Bethe–Salpeter approaches that can currently only be used for *static* calculations.

First principles molecular dynamics “involving excited states and nonadiabatic transitions” clearly has two aspects associated with it. First of all, it is necessary to be able to propagate nuclei using forces derived from an excited state potential energy surface. Secondly, interactions between two, several, or many electronic states are required due to the nonadiabatic couplings that arise if the Born–Oppenheimer approximation is *not* invoked. This imposes the following structure upon this review. Based on the Born–Oppenheimer approximation to the full (non-relativistic) Schrödinger equation for electrons and nuclei (Sec. 2.1.1), we derive the fundamental equations of molecular dynamics with classical nuclei in Sec. 2.1.2 in order to set the stage. Important first principles molecular dynamic methods for adiabatic ground state propagation are concisely reviewed in Sec. 2.2 and we refer to Ref. 11 for a more comprehensive presentation. In the following section, Sec. 3, practical techniques are presented allowing adiabatic propagation of a molecular system of the sort discussed above. At the heart of this review is Sec. 4. In its first part, Sec. 4.1, fundamental aspects of nonadiabatic dynamics are presented without, however, detailed reference to any specific electronic structure approach. Practical nonadiabatic *ab initio* molecular dynamics methods are then obtained by combining a particular approach to deal with nonadiabaticity with a particular electronic structure method. Several such combinations that have already been implemented in computer codes and applied to study the type of system specified above are discussed in Sec. 4.2. We close with a critical, however not entirely unbiased, discussion (Sec. 5) of the current state of research and offer some personal thoughts about the future in this “exciting” field.

2. Adiabatic Molecular Dynamics

2.1. Theoretical background

2.1.1. Born–Oppenheimer approximation

Let us begin by introducing our nomenclature and by reviewing some well-known basic relations within the Schrödinger formulation of quantum mechanics. A complete, nonrelativistic, description of a system of N atoms having the positions $\mathbf{R} = (\mathbf{R}_1, \mathbf{R}_2, \dots, \mathbf{R}_I, \dots, \mathbf{R}_N)$ with n electrons located at $\mathbf{r} = (\mathbf{r}_1, \mathbf{r}_2, \dots, \mathbf{r}_i, \dots, \mathbf{r}_n)$ is provided by the time-dependent Schrödinger equation

$$\mathcal{H}\Phi(\mathbf{r}, \mathbf{R}; t) = i\hbar \frac{\partial}{\partial t} \Phi(\mathbf{r}, \mathbf{R}; t) \quad (1)$$

with the total Hamiltonian

$$\mathcal{H}(\mathbf{r}, \mathbf{R}) = \mathcal{T}(\mathbf{R}) + \mathcal{T}(\mathbf{r}) + \mathcal{V}(\mathbf{R}) + \mathcal{V}(\mathbf{r}, \mathbf{R}) + \mathcal{V}(\mathbf{r}) \quad (2)$$

being the sum of kinetic energy of the atomic nuclei,

$$\mathcal{T}(\mathbf{R}) = -\frac{\hbar^2}{2} \sum_{I=1}^N \frac{\nabla_I^2}{M_I} \quad (3)$$

kinetic energy of the electrons,

$$\mathcal{T}(\mathbf{r}) = -\frac{\hbar^2}{2m_e} \sum_{i=1}^n \nabla_i^2 \quad (4)$$

internuclear repulsion,

$$\mathcal{V}(\mathbf{R}) = \frac{e^2}{4\pi\epsilon_0} \sum_{I=1}^{N-1} \sum_{J>I}^N \frac{Z_I Z_J}{|\mathbf{R}_I - \mathbf{R}_J|} \quad (5)$$

electronic — nuclear attraction,

$$\mathcal{V}(\mathbf{r}, \mathbf{R}) = -\frac{e^2}{4\pi\epsilon_0} \sum_{I=1}^N \sum_{i=1}^n \frac{Z_I}{|\mathbf{r}_i - \mathbf{R}_I|} \quad (6)$$

and interelectronic repulsion,

$$\mathcal{V}(\mathbf{r}) = \frac{e^2}{4\pi\epsilon_0} \sum_{i=1}^{n-1} \sum_{j>i}^n \frac{1}{|\mathbf{r}_i - \mathbf{r}_j|}. \quad (7)$$

Here, M_I and Z_I denote the mass and atomic number of nucleus I ; m_e and e are the electronic mass and elementary charge, and ϵ_0 is the permittivity of vacuum. The nabla operators ∇_I and ∇_i act on the coordinates of nucleus I and electron i , respectively.

Defining the partial electronic Hamiltonian for fixed nuclei (i.e. the clamped-nuclei part of \mathcal{H}) as

$$\mathcal{H}_{\text{el}}(\mathbf{r}, \mathbf{R}) = \mathcal{T}(\mathbf{r}) + \mathcal{V}(\mathbf{R}) + \mathcal{V}(\mathbf{r}, \mathbf{R}) + \mathcal{V}(\mathbf{r}) \quad (8)$$

we rewrite the total Hamiltonian as

$$\mathcal{H}(\mathbf{r}, \mathbf{R}) = \mathcal{T}(\mathbf{R}) + \mathcal{H}_{\text{el}}(\mathbf{r}, \mathbf{R}). \quad (9)$$

Let us suppose the solutions of the time-independent (electronic) Schrödinger equation,

$$\mathcal{H}_{\text{el}}(\mathbf{r}, \mathbf{R})\Psi_k(\mathbf{r}, \mathbf{R}) = E_k(\mathbf{R})\Psi_k(\mathbf{r}, \mathbf{R}) \quad (10)$$

are known for clamped nuclei. Furthermore, the spectrum of $\mathcal{H}_{\text{el}}(\mathbf{r}, \mathbf{R})$ is assumed to be discrete and the eigenfunctions orthonormalized

$$\int_{-\infty}^{\infty} \Psi_k^*(\mathbf{r}, \mathbf{R})\Psi_l(\mathbf{r}, \mathbf{R})d\mathbf{r} \equiv \langle \Psi_k | \Psi_l \rangle = \delta_{kl}. \quad (11)$$

The total wavefunction Φ can be expanded in terms of the eigenfunctions of \mathcal{H}_{el} since these form a complete set

$$\Phi(\mathbf{r}, \mathbf{R}; t) = \sum_l \Psi_l(\mathbf{r}, \mathbf{R})\chi_l(\mathbf{R}, t). \quad (12)$$

Insertion of this so-called Born–Oppenheimer ansatz into the time-dependent Schrödinger Eq. (1) followed by multiplication from the left by $\Psi_k^*(\mathbf{r}, \mathbf{R})$ and integration over the electronic coordinates leads to a set of coupled differential equations

$$[\mathcal{T}(\mathbf{R}) + E_k(\mathbf{R})]\chi_k + \sum_l C_{kl}\chi_l = i\hbar \frac{\partial}{\partial t} \chi_k \quad (13)$$

where the coupling operator C_{kl} is defined as

$$C_{kl} \equiv \langle \Psi_k | \mathcal{T}(\mathbf{R}) | \Psi_l \rangle - \sum_I \frac{\hbar^2}{M_I} \langle \Psi_k | \nabla_I | \Psi_l \rangle \nabla_I. \quad (14)$$

The diagonal term C_{kk} represents a correction to the (adiabatic) eigenvalue E_k of the electronic Schrödinger Eq. (10). The well-known adiabatic approximation is obtained by taking into account only these diagonal terms, $C_{kk} \equiv \langle \Psi_k | \mathcal{T}(\mathbf{R}) | \Psi_k \rangle$, which results in complete decoupling

$$[\mathcal{T}(\mathbf{R}) + E_k(\mathbf{R}) + C_{kk}(\mathbf{R})]\chi_k = i\hbar \frac{\partial}{\partial t} \chi_k \quad (15)$$

of the exact set of differential Eqs. (13). This, in turn, implies that nuclear motion proceeds without

changing the quantum state of the electronic subsystem during time evolution and, correspondingly, the wavefunction (12) is reduced to a single term

$$\Phi(\mathbf{r}, \mathbf{R}; t) \approx \Psi_k(\mathbf{r}, \mathbf{R})\chi_k(\mathbf{R}, t) \quad (16)$$

being the direct product of an electronic and a nuclear wavefunction. The ultimate simplification consists in neglecting also the diagonal coupling terms

$$[\mathcal{T}(\mathbf{R}) + E_k(\mathbf{R})]\chi_k = i\hbar \frac{\partial}{\partial t} \chi_k \quad (17)$$

which defines the Born–Oppenheimer (or clamped nuclei) approximation, see Refs. 74 and 75 for more in-depth discussions. Let us stress that we have ignored in our simple presentation possible complications through the geometric (“Berry”) phase and we refer the reader to Ref. 76 for an excellent review on the subtleties of this subject.

For a great number of physical situations the Born–Oppenheimer approximation can be safely applied. On the other hand, there are many important chemical phenomena like, for instance, charge transfer and photoisomerization reactions, whose very existence is due to the inseparability of electronic and nuclear motion. Inclusion of nonadiabatic effects will be the subject of Sec. 4.

2.1.2. Classical nuclei and trajectories

In principle, solving (17) yields a complete description of nuclear (quantum) dynamics within the Born–Oppenheimer approximation. However, for a system with many degrees of freedom, quantum mechanical treatment of the nuclei becomes computationally prohibitive. For this reason, the classical approximation is often imposed. Separating the modulus and the phase of the nuclear wavefunction in the k th electronic state,

$$\chi_k(\mathbf{R}, t) = A_k(\mathbf{R}, t)e^{\frac{i}{\hbar}S_k(\mathbf{R}, t)} \quad (18)$$

where A_k and S_k are real, one obtains from (17) for all real terms

$$\frac{\partial S_k}{\partial t} = \sum_I \frac{\hbar^2}{2M_I} \frac{\nabla_I^2 A_k}{A_k} - \sum_I \frac{(\nabla_I S_k)^2}{2M_I} - E_k \quad (19)$$

and for all imaginary terms

$$\frac{\partial A_k}{\partial t} = - \sum_I \frac{(\nabla_I A_k)(\nabla_I S_k)}{M_I} - \sum_I \frac{A_k(\nabla_I^2 S_k)}{2M_I}. \quad (20)$$

Multiplying by $2A_k$ from the left, (20) may be rewritten as

$$\frac{\partial A_k^2}{\partial t} + \sum_I \frac{\nabla_I(A_k^2 \nabla_I S_k)}{M_I} = 0 \quad (21)$$

which is easily identified as the continuity equation, where $P = A_k^2$ and $\mathbf{J}_I = A_k^2(\nabla_I S_k)/M_I$ are the probability density and the current density in the k th electronic state, respectively.

In the classical limit ($\hbar = 0$), (21) remains unchanged, whereas (19) becomes

$$\frac{\partial S_k}{\partial t} = - \sum_I \frac{(\nabla_I S_k)^2}{2M_I} - E_k. \quad (22)$$

Recognizing that the nuclear velocities are given by

$$\dot{\mathbf{R}}_I = \frac{\mathbf{J}_I}{P} = \frac{\nabla_I S_k}{M_I} \quad (23)$$

one obtains the well-known Hamilton–Jacobi equation of classical mechanics

$$\frac{\partial S_k}{\partial t} = -(T_k + E_k) = -E^{\text{tot}} = \text{const.} \quad (24)$$

where

$$T_k = \sum_I \frac{1}{2} M_I \dot{\mathbf{R}}_I^2 \quad (25)$$

is the classical kinetic energy of the nuclei and E^{tot} is the (constant) total energy. Taking the gradient of (24) finally yields Newton’s equation of motion

$$M_I \ddot{\mathbf{R}}_I = -\nabla_I E_k \quad (26)$$

for classical nuclear motion in the k th electronic state.

2.2. Ground state methods

The approximations presented in the previous two subsections form the basis of conventional molecular dynamics. Thus, in principle, a classical trajectory calculation merely amounts to integrating Newton’s equations of motion (26). In practice, however, this deceptively simple task is complicated by the fact that the stationary Schrödinger Eq. (10) cannot be solved exactly for any many-electron system. The potential energy surface therefore has to be approximated using *ab initio* electronic structure methods or empirical interaction potentials (so-called force-field molecular dynamics, Refs. 1 and 77). The latter is

problematic, because empirical parameters obtained for a specific system under certain environmental conditions are not generally transferable to other systems under different conditions. Moreover, the use of pair potentials is dangerous, since many-body effects are not properly taken into account. Many-body interaction potentials for systems with many different chemical elements, on the other hand, cannot be determined accurately. The most serious limitation of empirical potentials, however, is their inability to account for chemical reactions, i.e. bond breaking and formation. When it comes to computing a *global* potential energy surface by *ab initio* calculations an additional difficulty is the “dimensionality bottleneck”, i.e. the strong increase of the number of points needed in order to span the surface as the number of nuclei increases, see Ref. 11 for further discussion.

In the following, we shall focus on first principles molecular dynamics methods. Due to the high computational cost associated with *ab initio* electronic structure calculations of large molecules, computation of the entire potential energy surface prior to the molecular dynamics simulation is best avoided. A more efficient alternative is the evaluation of electronic energy and nuclear forces “on the fly” at each step along the trajectory. In the so-called Born–Oppenheimer implementation of such a scheme,¹¹ the nuclei are propagated by integration of (26), where the exact energy E_k is replaced with the eigenvalue, \tilde{E}_k , of some approximate electronic Hamiltonian, $\tilde{\mathcal{H}}_{\text{el}}$, which is calculated at each time step. For the electronic ground state, i.e. $k = 0$, the use of Kohn–Sham (KS) density functional theory^{70,71} has become increasingly popular.

In order to further increase computational efficiency, Car and Parrinello have introduced a technique to bypass the need for wavefunction optimization at each molecular dynamics step.^{10,11} Instead, the molecular wavefunction is dynamically propagated along with the atomic nuclei according to the equations of motion

$$M_I \ddot{\mathbf{R}}_I = -\nabla_I \langle \Psi_k | \tilde{\mathcal{H}}_{\text{el}} | \Psi_k \rangle \quad (27)$$

$$\mu_i \ddot{\psi}_i = -\frac{\delta}{\delta \psi_i^*} \langle \Psi_k | \tilde{\mathcal{H}}_{\text{el}} | \Psi_k \rangle + \sum_j \lambda_{ij} \psi_j \quad (28)$$

where the KS one-electron orbitals ψ_i are kept orthonormal by the Lagrange multipliers λ_{ij} . These are the Euler–Lagrange equations

$$\frac{d}{dt} \frac{\partial \mathcal{L}}{\partial \dot{q}} = \frac{\partial \mathcal{L}}{\partial q}, \quad (q = \mathbf{R}_I, \psi_i^*) \quad (29)$$

for the Car–Parrinello Lagrangian¹⁰

$$\mathcal{L} = \sum_I \frac{1}{2} M_I \dot{\mathbf{R}}_I^2 + \sum_i \frac{1}{2} \mu_i \langle \dot{\psi}_i | \dot{\psi}_i \rangle - \langle \Psi_k | \tilde{\mathcal{H}}_{\text{el}} | \Psi_k \rangle + \sum_{ij} \lambda_{ij} (\langle \psi_i | \psi_j \rangle - \delta_{ij}) \quad (30)$$

that is formulated here for an arbitrary electronic state Ψ_k , an arbitrary electronic Hamiltonian $\tilde{\mathcal{H}}_{\text{el}}$, and an arbitrary basis (i.e. without invoking the Hellmann–Feynman theorem).

3. Excited State Molecular Dynamics

3.1. Wavefunction-based methods

Extending adiabatic *ab initio* molecular dynamics to the propagation of classical nuclei in a single non-interacting excited state is straightforward in the framework of wavefunction-based methods such as Hartree–Fock,^{78–88} generalized valence bond (GVB),^{89–93} multi-configuration self-consistent field (MCSCF),⁷⁹ complete active space SCF (CASSCF),^{82,94,95} or full configuration interaction (FCI)⁹⁶ approaches. However, these methods are computationally rather demanding — even given present-day methods, algorithms, and hardware. Recently, an approximate Hartree–Fock treatment was implemented in order to propagate a seven-atom cluster in its first excited state.⁹⁷

3.2. Energy penalty functional method

Owing to their favorable scaling and low computational demand, density functional methods may be applied to considerably larger systems than the wavefunction-based approaches discussed in the previous subsection. However, Hohenberg–Kohn–Sham^{72,73} density functional theory in its original form only provides the electronic ground state.^{70,71} The pioneering paper extending Car–Parrinello-type simulations to selected excited states was based on adding a suitable “dispersion functional” to the usual Kohn–Sham functional.^{98–100} This energy penalty contribution “stabilizes” some electronic state by converting a saddle point of the original Kohn–Sham functional into a *local* minimum. The basic idea of this

approach^{99,100} is best motivated by first discussing the generic problem

$$E[\Psi] = \langle \Psi | \mathcal{H} | \Psi \rangle \quad (31)$$

where Ψ_0 is the ground-state wavefunction obtained from the *absolute* minimum of the energy functional $E[\Psi]$ satisfying $\langle \Psi | \Psi \rangle = 1$, and for simplicity it is assumed that Ψ is a real function. However, E is stationary at all eigenstates Ψ_k , i.e. excited states $k > 0$ are saddle points of E and thus cannot be obtained by its minimization. Considering instead of the first moment (31) of the Hamiltonian its variance

$$\Delta[\Psi] = \{ \langle \Psi | \mathcal{H}^2 | \Psi \rangle - \langle \Psi | \mathcal{H} | \Psi \rangle^2 \} \quad (32)$$

it is observed that this functional is non-negative and vanishes at all eigenstates, which implies that excited states are *local* minima of $\Delta[\Psi]$. Thus, the modification

$$\tilde{E}[\Psi] = E[\Psi] + \tilde{\Lambda} \{ \langle \Psi | \mathcal{H}^2 | \Psi \rangle - \langle \Psi | \mathcal{H} | \Psi \rangle^2 \} \quad (33)$$

with $\tilde{\Lambda} > 0$ leads to a functional that remains stationary for all eigenstates Ψ_k . In addition, any excited state Ψ_k is a *local* minimum of \tilde{E} if $\tilde{\Lambda} > (E[\Psi_k] - E[\Psi_0])^{-1}$. Thus, the dispersion contribution Δ can be viewed as some sort of a “harmonic confining potential” that causes an (additional) energy penalty if the system is not in one of its eigenstates. The barrier height separating the various local minima and thus the different excited states is controlled by $\tilde{\Lambda}$. Thus, the closer the energy levels the larger $\tilde{\Lambda}$ has to be chosen in order to create a sufficient separation.

The generalization of this idea within the framework of density functional theory leads to the following *ad hoc* modification of the Kohn–Sham functional

$$\tilde{E}[\{\psi_i\}] = E^{\text{KS}}[\{\psi_i\}] + \tilde{\Lambda} \left\{ \sum_i^{\text{occ}} \langle \psi_i | (\mathcal{H}_{\text{KS}}^2 | \psi_i \rangle - \sum_{i,j}^{\text{occ}} \langle \psi_i | \mathcal{H}_{\text{KS}} | \psi_j \rangle \langle \psi_j | \mathcal{H}_{\text{KS}} | \psi_i \rangle \right\} \quad (34)$$

which is now an orbital-dependent density functional that can be minimized for various states; the summation is over all occupied Kohn–Sham orbitals ψ_i . Having defined a suitable functional (34), the respective Car–Parrinello equations of motion

$$M_I \ddot{\mathbf{R}}_I = -\frac{\partial \tilde{E}}{\partial \mathbf{R}_I} \quad (35)$$

$$\mu \ddot{\psi}_i = -\frac{\delta \tilde{E}}{\delta \psi_i^*} + \sum_j \lambda_{ij} \psi_j = -\mathcal{H}_{\text{KS}} \psi_i + \sum_j \lambda_{ij} \psi_j - \tilde{\Lambda} \left\{ \mathcal{H}_{\text{KS}}^2 |\psi_i\rangle - 2 \sum_j \mathcal{H}_{\text{KS}} |\psi_j\rangle \langle \psi_j | \mathcal{H}_{\text{KS}} | \psi_i \rangle \right\} \quad (36)$$

for both electrons and nuclei can be derived as usual, see for instance (29). For the latter, one can make use of the Hellmann–Feynman theorem within a plane-wave Car–Parrinello approach including, of course, the penalty term, see Sec. 2.5 of Ref. 11 for a detailed discussion of this issue. For this approach to work the penalty term $\propto \tilde{\Lambda}$ has to be sufficiently large in order to stabilize a given excited state sufficiently with respect to neighboring (local) minima in the presence of fluctuations.

This idea seems closely related to the modified Ritz variational principle for excited states¹⁰¹ and its extension to density functional theory.¹⁰² However, one should keep in mind Lieb’s theorem (1985) that there exists no *universal* variational density functional procedure yielding an *individual* excited state, see Sec. 9.2 in Ref. 70 for a more detailed discussion of these issues.

This penalty functional approach to performing first principles simulations in a particular excited state was used successfully to study the self-trapping of a valence biexciton in diamond within LDA;¹⁰³ see Sec. 4 of Ref. 99 for more methodological details. In general it might be a practical problem to deliberately select a particular excited state. This was achieved in Ref. 99 by constructing trial initial states that were “close” to a particular excitonic state. Furthermore, fixing the strength $\tilde{\Lambda}$ of the confining potential might turn out to be a delicate task. If it is too weak the resulting local minimum is too shallow and thus the system might easily switch from one state to another. In particular, it might relax from the first excited state into the ground state due to fluctuations occurring during a dynamical simulation. On the other hand, in real applications the limit of large $\tilde{\Lambda}$ might lead to artificial distortions of the Kohn–Sham potential energy surface, E^{KS} , as generated by the new density functional \tilde{E} , which could easily produce unphysical states. Finally, it should be kept in mind that available local or semilocal density functionals are not expected to lead to “correct” excited states, but they might yield reasonable approximations in some cases.⁹⁹

3.3. Restricted open-shell Kohn–Sham functional

A class of alternative approaches to excited states in the spirit of density functional theory in its Kohn–Sham formulation^{70,71} is based on imposing additional symmetry restrictions. Several extensions for computing atomic and molecular multiplet structures by incorporating spatial or/and spin symmetry have been proposed.^{104–115} We shall expand here on the restricted open-shell Kohn–Sham (ROKS) method introduced by Frank and coworkers,¹¹⁰ since it is the only approach that has already been used in adiabatic^{110,116,117} and nonadiabatic¹¹⁸ excited state molecular dynamics simulations.

Similar to restricted open-shell Hartree–Fock theory, the central idea of the ROKS approach is to impose symmetry constraints on the many-electron wavefunction by constructing a symmetry-adapted multi-determinantal wavefunction,

$$\Psi^S = \sum_M a_M \Phi_M \quad (37)$$

from spin-restricted single Slater determinants (“microstates”), Φ_M . Following Roothaan,¹¹⁹ the expansion coefficients, a_M , are chosen to be the Clebsch–Gordon coefficients for a given symmetry. The energy is then given by (Refs. 113–115)

$$E^S = \sum_M c_M E(\Phi_M) \quad (38)$$

where

$$\sum_M c_M = 1. \quad (39)$$

The ROKS method has been formulated explicitly in Ref. 110 for the lowest excited singlet state, S_1 , but generalizations to arbitrary multiplets have been proposed in the literature.^{111–115}

Suppose we are dealing with a closed-shell ground state system with n electrons occupying $l = n/2$ spin-restricted orbitals (having the same spatial part for both spin up (α) and spin down (β) electrons).

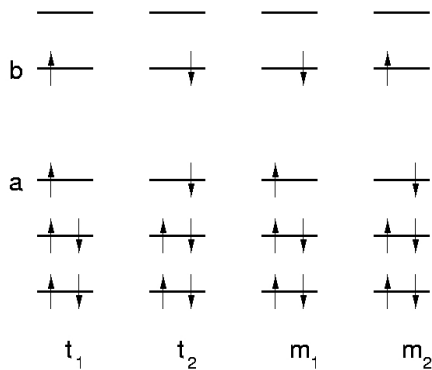


Fig. 1. Four possible determinants $|t_1\rangle$, $|t_2\rangle$, $|m_1\rangle$ and $|m_2\rangle$ as a result of the promotion of a single electron from the HOMO to the LUMO of a closed shell ground state system, see text for further details. Adapted from Ref. 110.

Promotion of one electron from the HOMO to the LUMO gives rise to four possible spin configurations (see Fig. 1 for a sketch) of the two unpaired electrons. The two determinants with parallel unpaired spins, $|t_1\rangle$ and $|t_2\rangle$, are energetically degenerate triplets, t , whereas the two antiparallel spin configurations, $|m_1\rangle$

and $|m_2\rangle$, are not eigenfunctions of the total spin operator, \mathcal{S}^2 . In fact, they are energetically degenerate, equal mixtures, m , of the spin-adapted two-configurational singlet,

$$|s_1\rangle = \frac{1}{\sqrt{2}}\{|m_1\rangle + |m_2\rangle\} \quad (40)$$

and triplet,

$$|t_3\rangle = \frac{1}{\sqrt{2}}\{|m_1\rangle - |m_2\rangle\} \quad (41)$$

wavefunctions (“spin contamination”). By inverting the energy expression for the mixed state, m ,

$$E(m) = \frac{1}{2}(E(s_1) + E(t)) \quad (42)$$

one obtains the energy of the S_1 state [cf. Eq. (38)]

$$E(s_1) = 2E(m) - E(t). \quad (43)$$

In terms of Kohn–Sham density functional theory the energies of the mixed and triplet determinants can be written as¹¹⁰

$$E(m) \equiv E_m^{\text{KS}}[\{\psi_i\}] = T_s[n] + \int d\mathbf{r} V_{\text{ext}}(\mathbf{r})n(\mathbf{r}) + \frac{1}{2} \int d\mathbf{r} V_{\text{H}}(\mathbf{r})n(\mathbf{r}) + E_{\text{xc}}[n_m^\alpha, n_m^\beta] \quad (44)$$

$$E(t) \equiv E_t^{\text{KS}}[\{\psi_i\}] = T_s[n] + \int d\mathbf{r} V_{\text{ext}}(\mathbf{r})n(\mathbf{r}) + \frac{1}{2} \int d\mathbf{r} V_{\text{H}}(\mathbf{r})n(\mathbf{r}) + E_{\text{xc}}[n_t^\alpha, n_t^\beta] \quad (45)$$

where a *single* set of restricted KS orbitals $\{\psi_i\}$ is used for both determinants, m and t . As a consequence, the total density,

$$n(\mathbf{r}) = n_m^\alpha(\mathbf{r}) + n_m^\beta(\mathbf{r}) = n_t^\alpha(\mathbf{r}) + n_t^\beta(\mathbf{r}) \quad (46)$$

is, of course, identical for both the m and the t determinants whereas their spin densities clearly differ (see Fig. 2). Thus, in the energy functionals (44) and (45), kinetic, external, and Hartree energies are identical by construction. Therefore, the exchange-correlation functional E_{xc} is solely responsible for any differences.

Having defined a density functional for the first excited singlet state the corresponding Kohn–Sham equations are obtained by varying (43) using (44) and (45) subject to the orthonormality constraint $\sum_{i,j=1}^{l+1} \lambda_{ij}(\langle\psi_i|\psi_j\rangle - \delta_{ij})$. Following this procedure the equation for the doubly occupied orbitals $i = 1, \dots, l - 1$ reads

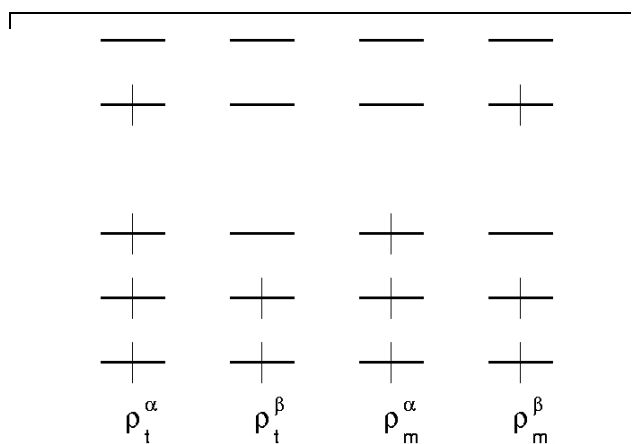


Fig. 2. Four patterns of spin densities n_t^α , n_t^β , n_m^α , and n_m^β corresponding to the two spin-restricted determinants $|t\rangle$ and $|m\rangle$ sketched in Fig. 1, see text for further details. Adapted from Ref. 110.

$$\left\{ -\frac{1}{2}\nabla^2 + V_{\text{H}}(\mathbf{r}) + V_{\text{ext}}(\mathbf{r}) + V_{\text{xc}}^{\alpha}[n_m^{\alpha}(\mathbf{r}), n_m^{\beta}(\mathbf{r})] + V_{\text{xc}}^{\beta}[n_m^{\alpha}(\mathbf{r}), n_m^{\beta}(\mathbf{r})] \right. \\ \left. - \frac{1}{2}V_{\text{xc}}^{\alpha}[n_t^{\alpha}(\mathbf{r}), n_t^{\beta}(\mathbf{r})] - \frac{1}{2}V_{\text{xc}}^{\beta}[n_t^{\alpha}(\mathbf{r}), n_t^{\beta}(\mathbf{r})] \right\} \psi_i(\mathbf{r}) = \sum_{j=1}^{l+1} \lambda_{ij} \psi_j(\mathbf{r}) \quad (47)$$

whereas

$$\left\{ \frac{1}{2} \left[-\frac{1}{2}\nabla^2 + V_{\text{H}}(\mathbf{r}) + V_{\text{ext}}(\mathbf{r}) \right] + V_{\text{xc}}^{\alpha}[n_m^{\alpha}(\mathbf{r}), n_m^{\beta}(\mathbf{r})] - \frac{1}{2}V_{\text{xc}}^{\alpha}[n_t^{\alpha}(\mathbf{r}), n_t^{\beta}(\mathbf{r})] \right\} \psi_a(\mathbf{r}) = \sum_{j=1}^{l+1} \lambda_{aj} \psi_j(\mathbf{r}) \quad (48)$$

and

$$\left\{ \frac{1}{2} \left[-\frac{1}{2}\nabla^2 + V_{\text{H}}(\mathbf{r}) + V_{\text{ext}}(\mathbf{r}) \right] + V_{\text{xc}}^{\beta}[n_m^{\alpha}(\mathbf{r}), n_m^{\beta}(\mathbf{r})] - \frac{1}{2}V_{\text{xc}}^{\beta}[n_t^{\alpha}(\mathbf{r}), n_t^{\beta}(\mathbf{r})] \right\} \psi_b(\mathbf{r}) = \sum_{j=1}^{l+1} \lambda_{bj} \psi_j(\mathbf{r}) \quad (49)$$

are two *different* equations for the two singly-occupied open-shell orbitals a and b , respectively (see Fig. 1). Note that these Kohn–Sham-like equations feature orbital-dependent exchange-correlation potentials,

$$V_{\text{xc}}^{\sigma}[n_M^{\alpha}, n_M^{\beta}] = \delta E_{\text{xc}}[n_M^{\alpha}, n_M^{\beta}] / \delta n_M^{\sigma} \quad (50)$$

where $\sigma = \alpha, \beta$ and $M = m, t$.

The set of Eqs. (47)–(49) could be solved by diagonalization of the corresponding “restricted open-shell Kohn–Sham Hamiltonian” or alternatively by direct minimization of the associated total energy functional. The algorithm proposed in Ref. 120, which allows to properly and efficiently minimize such orbital-dependent functionals including the orthonormality constraints, has been implemented in the CPMD package.¹²¹ Based on this minimization technique Born–Oppenheimer molecular dynamics simulations can be performed in the first excited singlet state.^{110,116} The ROKS method has also been employed in Car–Parrinello molecular dynamics calculations^{117,118} according to the general equations of motion (27) and (28) from Sec. 2.2.

Excitation energies and excited state optimized molecular structures obtained using the ROKS method have been found to be quite accurate (on the scale given by typical time-dependent density functional results or ground-state density functional calculations for the structures) in the case of $n \rightarrow \pi^*$ transitions.¹¹⁰ The ROKS results generally appear to be less reliable for electronic states that are energetically not well isolated.¹¹⁷ This observation has been made in particular for many $\pi \rightarrow \pi^*$ excitations.¹¹⁷

In summary, the ROKS method takes care of the spin symmetry of the molecular wavefunction through the two-determinantal ansatz for the S_1 wavefunction. In a single determinant, unrestricted Kohn–Sham ansatz, the symmetry restriction would have to be built into the exchange-correlation functional. Therefore, the ROKS method puts less strain on the functional. In addition, we would like to stress again the fact that the ROKS energy functional is indeed an orbital functional (akin to the OEP/OPM^{122,123} family of functionals) and does not merely depend on the local density and its derivatives.

3.4. Time-dependent density functional response theory

Time-dependent density functional theory (TDDFT)^{71,124–126} linear response calculations^{127–129} of molecular properties such as excitation spectra and dynamic polarizabilities have become a standard tool in quantum chemistry over the past few years.^{130–133} It has been demonstrated^{132,133} that mean errors of a fraction of an electron Volt can be achieved for TDDFT molecular excitation energies when accurate exchange-correlation potentials, V_{xc} , are used. Correct asymptotic long-range behavior of V_{xc} , in particular, has been shown to be crucial for a high quality description of Rydberg transitions.

Extensions of the TDDFT method to adiabatic excited state and multi-state nonadiabatic dynamics are highly desirable, because practically the entire electronic spectrum of a given molecule is reliably

obtained from a single calculation at comparatively low computational expense. Calculation of excited state nuclear gradients in TDDFT, however, is not straightforward. Nevertheless, the progress currently made in this field^{134–136} promises to have a massive impact on *ab initio* excited state MD.

A formalism that makes it possible to perform Car–Parrinello MD simulations on excited state potential energy surfaces obtained by TDDFT has been presented recently.¹³⁷ In the following, we shall briefly summarize the central ideas.

In the framework of TDDFT the excitation energies $\omega = \omega_k = E_k^{\text{KS}} - E_0^{\text{KS}}$ are the poles of the

density response function; in practice they can be calculated by solving the non-Hermitian eigenvalue problem

$$\begin{pmatrix} \mathbf{A} & \mathbf{B} \\ \mathbf{B} & \mathbf{A} \end{pmatrix} \begin{pmatrix} \mathbf{X} \\ \mathbf{Y} \end{pmatrix} = \omega \begin{pmatrix} \mathbf{X} \\ -\mathbf{Y} \end{pmatrix} \quad (51)$$

with

$$A_{ia\sigma,jb\tau} = \delta_{\sigma\tau} \delta_{ij} \delta_{ab} (\epsilon_{a\sigma} - \epsilon_{i\sigma}) + K_{ia\sigma,jb\tau} \quad (52)$$

$$B_{ia\sigma,jb\tau} = K_{ia\sigma,bj\tau}. \quad (53)$$

The coupling matrix \mathbf{K} is given by

$$\begin{aligned} K_{ia\sigma,jb\tau} = & \int d\mathbf{r} \int d\mathbf{r}' \psi_{i\sigma}(\mathbf{r}) \psi_{a\sigma}(\mathbf{r}) \frac{1}{|\mathbf{r} - \mathbf{r}'|} \psi_{j\tau}(\mathbf{r}') \psi_{b\tau}(\mathbf{r}') \\ & + \int d\mathbf{r} \int d\mathbf{r}' \psi_{i\sigma}(\mathbf{r}) \psi_{a\sigma}(\mathbf{r}) f_{\text{xc}}^{\sigma\tau}(\mathbf{r}, \mathbf{r}', \omega) \psi_{j\tau}(\mathbf{r}') \psi_{b\tau}(\mathbf{r}') \end{aligned} \quad (54)$$

$\psi_{i\sigma}$ denoting the i th KS orbital (occupied orbitals are labeled i, j , unoccupied ones a, b) with spin σ ($\sigma = \alpha, \beta$) and the exchange-correlation kernel being defined as

$$f_{\text{xc}}^{\sigma\tau}(\mathbf{r}, t, \mathbf{r}', t') = \frac{\delta V_{\text{xc}}^{\sigma}(\mathbf{r}, t)}{\delta n^{\tau}(\mathbf{r}', t')}. \quad (55)$$

Using the adiabatic local density approximation (ALDA),¹²⁵ the exchange-correlation potential V_{xc}^{σ} can be replaced by the derivative of the exchange-

correlation energy, E_{xc} , with respect to the spin density n^{σ}

$$V_{\text{xc}}^{\sigma, \text{ALDA}}(\mathbf{r}, t) = \frac{\delta E_{\text{xc}}}{\delta n^{\sigma}(\mathbf{r})}. \quad (56)$$

In the spirit of Car–Parrinello MD one can write down a Lagrangian¹³⁷ describing the classical motion of KS orbitals $\{\psi_i\}$, response amplitudes \mathbf{X}, \mathbf{Y} , and atomic nuclei \mathbf{R} ,

$$\begin{aligned} \mathcal{L} = & \sum_I \frac{1}{2} M_I \dot{\mathbf{R}}_I^2 + \sum_i \frac{1}{2} \mu_i \langle \dot{\psi}_i | \dot{\psi}_i \rangle + \sum_k \sum_{ia\sigma} \frac{1}{2} \nu |\dot{X}_{ia\sigma}^k|^2 + \sum_k \sum_{ia\sigma} \frac{1}{2} \nu |\dot{Y}_{ia\sigma}^k|^2 \\ & - E_0^{\text{KS}} - \omega_k + \sum_{ij} \lambda_{ij} (\langle \psi_i | \psi_j \rangle - \delta_{ij}) + \sum_{kl} \Gamma_{kl} (\langle \mathbf{Z}_L^k | \mathbf{Z}_R^l \rangle - \delta_{kl}) \end{aligned} \quad (57)$$

where

$$\mathbf{Z}_L^k = \begin{pmatrix} \mathbf{X}^k \\ -\mathbf{Y}^k \end{pmatrix}, \quad \mathbf{Z}_R^k = \begin{pmatrix} \mathbf{X}^k \\ \mathbf{Y}^k \end{pmatrix} \quad (58)$$

ν is a fictitious mass associated with the response amplitudes, and the Γ_{kl} are Lagrange multipliers constraining the excited states to be orthonormal (for all other symbols see Sec. 2.2). From the Euler–Lagrange Eqs. (29), one obtains the equations of motions¹³⁷ for the one-electron orbitals,

$$\mu_i \ddot{\psi}_i = -\frac{\delta E_0^{\text{KS}}}{\delta \psi_i^*} + \sum_j \lambda_{ij} \psi_j \quad (59)$$

for the response amplitudes

$$\nu \begin{pmatrix} \ddot{\mathbf{X}} \\ \ddot{\mathbf{Y}} \end{pmatrix} = -\begin{pmatrix} \mathbf{A} & \mathbf{B} \\ \mathbf{B} & \mathbf{A} \end{pmatrix} \begin{pmatrix} \mathbf{X} \\ \mathbf{Y} \end{pmatrix} + \Gamma \begin{pmatrix} \mathbf{X} \\ -\mathbf{Y} \end{pmatrix} \quad (60)$$

and for the nuclei

$$M_I \ddot{\mathbf{R}}_I = -\nabla_I E_0^{\text{KS}} - \nabla_I \omega_k. \quad (61)$$

In the usual Car–Parrinello procedure, these equations would have to be solved using periodic boundary conditions in combination with a plane-wave basis set and pseudopotentials.¹¹ As a first step, it has been demonstrated¹³⁸ that static TDDFT calculations in this setup faithfully reproduce previous results obtained using atom centered basis sets.

4. Nonadiabatic Molecular Dynamics

4.1. Approaches to nonadiabatic dynamics

4.1.1. Introduction

The simplest and computationally least expensive way of incorporating nonadiabatic effects is by describing nuclear motion by classical mechanics and only the electrons quantum mechanically. In these so-called mixed quantum-classical approaches (often also referred to as semiclassical approaches),^{139–148} the atomic nuclei follow some trajectory $\mathbf{R}(t)$ while the electronic motion is captured by some time-dependent total wavefunction $\Psi(\mathbf{r}; t)$ satisfying the time-dependent electronic Schrödinger equation

$$\mathcal{H}_{\text{el}}(\mathbf{r}, \mathbf{R}(t))\Psi(\mathbf{r}; t) = i\hbar \frac{\partial}{\partial t} \Psi(\mathbf{r}; t). \quad (62)$$

Again, the total wavefunction is written as a linear combination of adiabatic eigenfunctions $\Psi_k(\mathbf{r}, \mathbf{R})$

$$\Psi(\mathbf{r}; t) = \sum_l a_l(t) \Psi_l(\mathbf{r}, \mathbf{R}) e^{-\frac{i}{\hbar} \int E_l(\mathbf{R}) dt} \quad (63)$$

that are solutions of the time-independent Schrödinger Eq. (10) for nuclei at positions \mathbf{R} at time t . Insertion of this ansatz into the time-dependent electronic Schrödinger Eq. (62) followed by multiplication from the left by $\Psi_k^*(\mathbf{r}, \mathbf{R})$ and integration over the electronic coordinates leads to a set of coupled differential equations

$$\dot{a}_k = - \sum_l a_l C_{kl} e^{-\frac{i}{\hbar} \int (E_l - E_k) dt} \quad (64)$$

where

$$C_{kl} \equiv \left\langle \Psi_k \left| \frac{\partial}{\partial t} \right| \Psi_l \right\rangle \quad (65)$$

are the nonadiabatic coupling elements. Making use of the chain rule, we can rewrite (65) as

$$C_{kl} = \dot{\mathbf{R}} \langle \Psi_l | \nabla | \Psi_k \rangle \equiv \dot{\mathbf{R}} \mathbf{d}_{kl} \quad (66)$$

where \mathbf{d}_{kl} is the nonadiabatic coupling vector.

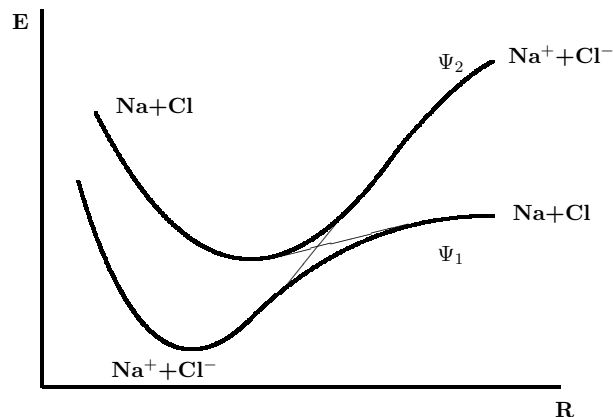


Fig. 3. Avoided crossing between the covalent and ionic adiabatic potential curves (solid lines) of NaCl (thin lines: crossing of diabatic states).

Integration of (64) yields the expansion coefficients $a_k(t)$ whose square modulus, $|a_k(t)|^2$, can be interpreted as the probability of finding the system in the adiabatic state k at time t .

We now want to develop a condition for the validity of the Born–Oppenheimer approximation based on qualitative arguments. For this purpose, we shall consider a two-state system. To illustrate the problem, Fig. 3 shows schematically the avoided crossing between the covalent and ionic potential energy curves of NaCl.^{149,150} As we can see, the adiabatic wavefunctions Ψ_1 and Ψ_2 change their character as the bond length is varied. The characteristic length, l , over which Ψ_1 and Ψ_2 change significantly clearly depends on the nuclear configuration \mathbf{R} ; in the vicinity of the NaCl avoided crossing, for instance, the character of the wavefunctions varies rapidly, whereas at large separations it remains more or less constant.

Division of the characteristic length l by the velocity of the nuclei, $\dot{R} = |\dot{\mathbf{R}}|$, at a particular configuration \mathbf{R} defines the passage time, τ_p , the system needs to travel the distance l around \mathbf{R}

$$\tau_p = \frac{l}{\dot{R}}. \quad (67)$$

In order for the Born–Oppenheimer (or the adiabatic) approximation to be valid, the electron cloud has to adjust instantly to the nuclear changes. The time scale characteristic of electronic motion can be obtained from the relation

$$\Delta E = |E_1 - E_2| = \hbar\omega \quad (68)$$

by taking the inverse transition frequency

$$\tau_e = \frac{1}{\omega} = \frac{\hbar}{\Delta E}. \quad (69)$$

The ratio

$$\xi = \frac{\tau_p}{\tau_e} = \frac{\Delta E l}{\hbar \dot{R}} \quad (70)$$

is the so-called Massey parameter.^{139,140,151,152} For values $\xi \gg 1$, i.e. large energy gaps ΔE and small velocities \dot{R} , nonadiabatic effects are negligible. In this case, if the system is prepared in some pure adiabatic state k at time $t = 0$ (i.e. $|a_k(0)|^2 = 1$), the right hand side of (64) will be zero at all times and the wavefunction expansion (63) can be replaced by a single term

$$\Psi(\mathbf{r}; t) = \Psi_k(\mathbf{r}, \mathbf{R}) e^{-\frac{i}{\hbar} \int E_k(\mathbf{R}) dt}. \quad (71)$$

The atomic nuclei are then propagated by solving Newton's Eqs. (26).

4.1.2. Mean-field (Ehrenfest) method

As we have discussed in the previous section, non-adiabaticity involves changes in the adiabatic state populations $|a_k|^2$ with changing nuclear configuration. Clearly, such a distortion of the electron cloud will, in turn, influence the nuclear trajectory. Although there are situations in which the impact of electronic non-adiabaticity on nuclear motion is negligible (e.g. for high energy collisions or small energy separations between adiabatic states where the so-called ‘‘Mott classical path method’’ works well), for many chemical systems it is of prime importance to properly incorporate electronic-nuclear feedback.^{144,145} The simplest way of doing this is to replace the adiabatic potential energy surface E_k in (26) by the energy expectation value

$$E_{\text{eff}} = \langle \Psi | \mathcal{H}_{\text{el}} | \Psi \rangle = \sum_k |a_k|^2 E_k \quad (72)$$

where we have used (63). Thus, the atoms evolve on an effective potential representing an average over the adiabatic states weighted by their state populations $|a_k|^2$ as illustrated in Fig. 4. The method is therefore referred to as mean-field (also known as Ehrenfest) approach.

It is instructive to derive an expression for the nuclear forces either from the gradient of (72) or using

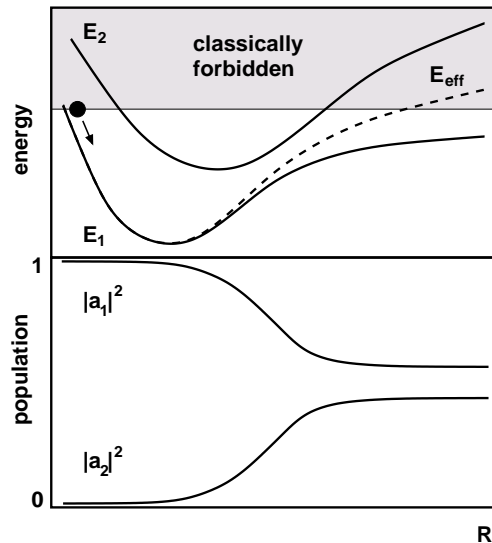


Fig. 4. Top: avoided crossing between two adiabatic potential energy surfaces, E_1 and E_2 , and effective potential, E_{eff} , on which the nuclei are propagated in the Ehrenfest method. In the asymptotic region (right) E_{eff} contains contributions from classically forbidden regions of E_2 . Bottom: corresponding adiabatic state populations $|a_1|^2$ and $|a_2|^2$. The system is prepared in state Ψ_1 initially with zero kinetic energy. Upon entering the coupling region state Ψ_2 is increasingly populated.

the Hellmann–Feynman theorem

$$\mathbf{F}_I = -\langle \Psi | \nabla_I \mathcal{H}_{\text{el}} | \Psi \rangle. \quad (73)$$

Opting for the latter, we start by writing down the relation

$$\begin{aligned} \nabla_I \langle \Psi_k | \mathcal{H}_{\text{el}} | \Psi_l \rangle &= \nabla_I E_k \delta_{kl} \end{aligned} \quad (74)$$

$$\begin{aligned} &= \langle \nabla_I \Psi_k | \mathcal{H}_{\text{el}} | \Psi_l \rangle + \langle \Psi_k | \nabla_I \mathcal{H}_{\text{el}} | \Psi_l \rangle \\ &\quad + \langle \Psi_k | \mathcal{H}_{\text{el}} | \nabla_I \Psi_l \rangle \end{aligned} \quad (75)$$

$$= \langle \Psi_k | \nabla_I \mathcal{H}_{\text{el}} | \Psi_l \rangle + (E_l - E_k) \mathbf{d}_{lk}^I \quad (76)$$

where we have defined the nonadiabatic coupling vectors, \mathbf{d}_{lk}^I , as

$$\mathbf{d}_{lk}^I = \langle \Psi_l | \nabla_I | \Psi_k \rangle \quad (77)$$

and used (10) together with the hermiticity of \mathcal{H}_{el}

$$\begin{aligned} \langle \Psi_k | \mathcal{H}_{\text{el}} | \nabla_I \Psi_l \rangle &= \langle \nabla_I \Psi_l | \mathcal{H}_{\text{el}} | \Psi_k \rangle^* = \langle \nabla_I \Psi_l | E_l \Psi_k \rangle^* \\ &= E_k (\mathbf{d}_{kl}^I)^* = -E_k \mathbf{d}_{lk}^I. \end{aligned} \quad (78)$$

Note that

$$(\mathbf{d}_{lk}^I)^* = -\mathbf{d}_{kl}^I \quad (79)$$

because

$$\begin{aligned} \nabla_I \langle \Psi_k | \Psi_l \rangle &= \nabla_I \delta_{kl} = 0 \end{aligned} \quad (80)$$

$$= \langle \nabla_I \Psi_k | \Psi_l \rangle + \langle \Psi_k | \nabla_I \Psi_l \rangle = (\mathbf{d}_{lk}^I)^* + \mathbf{d}_{kl}^I. \quad (81)$$

Equating the right hand sides of (74) and (76) one obtains after rearranging

$$\langle \Psi_k | \nabla_I \mathcal{H}_{\text{el}} | \Psi_l \rangle = \nabla_I E_k \delta_{kl} - (E_l - E_k) \mathbf{d}_{lk}^I. \quad (82)$$

The nuclear forces (73) are thus given by

$$\mathbf{F}_I = - \sum_k |a_k|^2 \nabla_I E_k + \sum_{k,l} a_k^* a_l (E_l - E_k) \mathbf{d}_{lk}^I. \quad (83)$$

Equation (83) illustrates the two contributions to the nuclear forces; the first term is simply the population-weighted average force over the adiabatic states, while the second term takes into account nonadiabatic changes of the adiabatic state occupations. We would

like to point out here that the nonadiabatic contributions to the nuclear forces are in the direction of the nonadiabatic coupling vectors \mathbf{d}_{lk}^I .

The Ehrenfest method has been applied with great success to a number of chemical problems including energy transfer at metal surfaces¹⁵³ and the study of excited state lifetimes and decay properties of organic molecules.¹⁵⁴ However, due to its mean-field character the method has some serious limitations. A system that was initially prepared in a pure adiabatic state will be in a mixed state when leaving the region of strong nonadiabatic coupling. In general, the pure adiabatic character of the wavefunction cannot be recovered even in the asymptotic regions of configuration space. In cases where the differences in the adiabatic potential energy landscapes are pronounced, it is clear that an average potential will be unable to describe all reaction channels adequately. In particular, if one is interested in a reaction branch whose occupation number is very small, the average path is likely to diverge from the “true trajectory”. Furthermore, the total wavefunction may contain significant

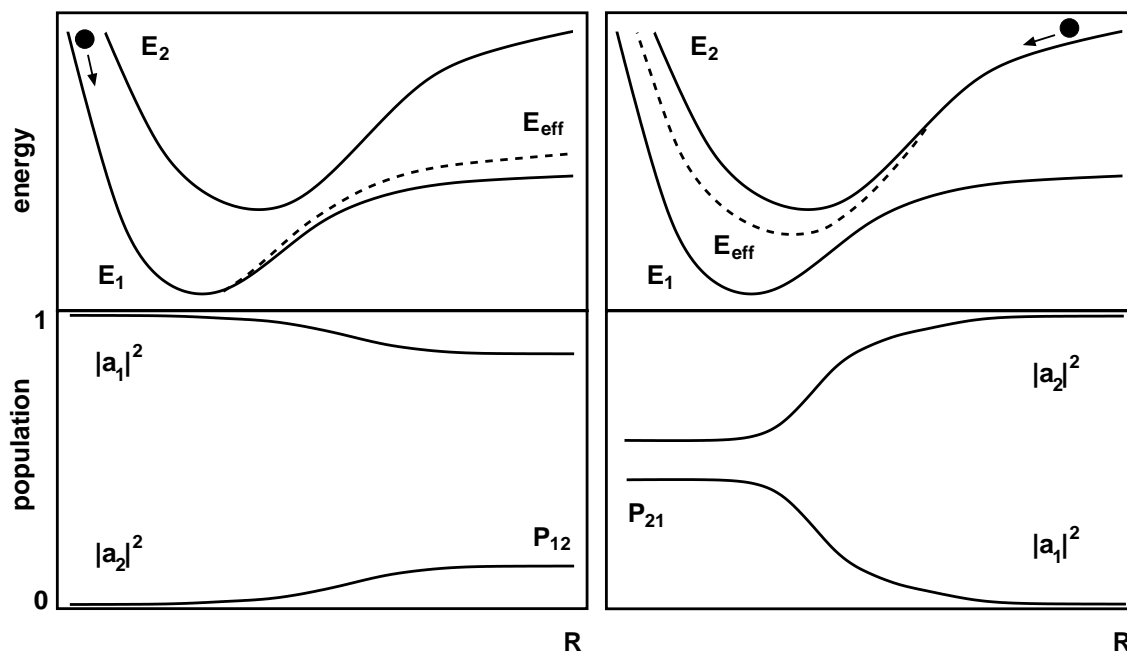


Fig. 5. Top left: forward path effective potential, E_{eff} , for two weakly coupled adiabatic potential energy surfaces, E_1 and E_2 . Bottom left: state occupations for a system initially prepared in state Ψ_1 . The final value of $|a_2|^2$ is equal to the transition probability P_{12} . Top right: backward path effective potential, E_{eff} , for two weakly coupled adiabatic potential energy surfaces, E_1 and E_2 . Bottom left: state occupations for a system initially prepared in state Ψ_2 . The final value of $|a_1|^2$ is equal to the transition probability P_{21} .

contributions from adiabatic states that are energetically inaccessible in classical mechanics, see Fig. 4.

Another severe drawback of the mean-field approach is illustrated in Fig. 5. The principle of microscopic reversibility demands that the forward path probability, $P_{12}^{\text{for}} = |a_2^{\text{final}}|^2$ for a system that was initially prepared in state Ψ_1 to end up in state Ψ_2 must be equal to the backward path probability, $P_{21}^{\text{back}} = |a_1^{\text{final}}|^2$ for a system that was initially prepared in state Ψ_2 to end up in state Ψ_1 . One can easily think of situations, like the one depicted in Fig. 5, for which the effective potentials for the forward and backward paths are very different, resulting also in different populations, $|a_k|^2$. The Ehrenfest method, therefore, violates microscopic reversibility.

It should be noted that the expansion of the total wavefunction in terms of (e.g. adiabatic) basis functions (63) is not a necessary requirement for the Ehrenfest method. The wavepacket Ψ could also be propagated numerically using directly the time-dependent Schrödinger Eq. (62). However, projection of Ψ onto the adiabatic states facilitates interpretation. Knowledge of the expansion coefficients, a_k , is also the key to refinements of the method such as the surface hopping technique, see the following Sec. 4.1.3.

4.1.3. Surface hopping

We have argued above that after exiting a well localized nonadiabatic coupling region it is unphysical for nuclear motion to be governed by a mixture of adiabatic states. Rather it would be desirable that in asymptotic regions the system evolves on a pure adiabatic potential energy surface. This idea is fundamental to the surface hopping approach. Instead of calculating “the best” (i.e. state-averaged) path like in the Ehrenfest method, the surface hopping technique involves an ensemble of trajectories (i.e. many different paths). At any moment in time, the system is propagated on some pure adiabatic state Ψ_k , which is selected according to its state population $|a_k|^2$. Changing adiabatic state occupations can thus result in nonadiabatic transitions between different adiabatic potential energy surfaces, see Fig. 6. The ensemble averaged number of trajectories evolving on adiabatic state k at any time is equal to its occupation number $|a_k|^2$.

In the original formulation of the surface hopping method by Tully and Preston,¹⁴¹ switches between

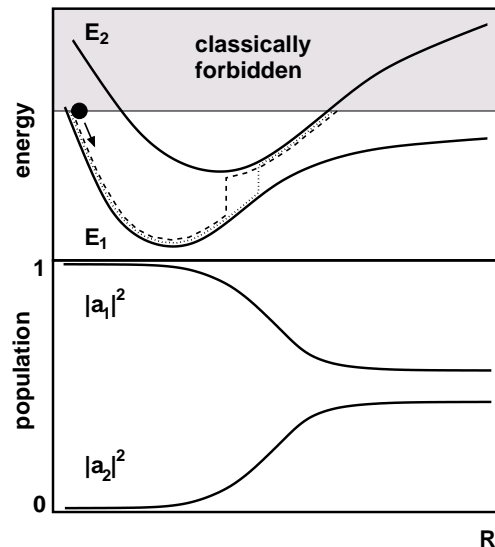


Fig. 6. Top: avoided crossing between two adiabatic potential energy surfaces, E_1 and E_2 , and two typical forward surface hopping trajectories (dashed and dotted lines). Nonadiabatic transitions are most likely to occur in the coupling region. Bottom: corresponding adiabatic state populations $|a_1|^2$ and $|a_2|^2$. The system is prepared to be in state Ψ_1 initially with zero kinetic energy. Upon entering the coupling region state Ψ_2 is increasingly populated.

adiabatic states were allowed only at certain locations defined prior to the simulation. Tully¹⁴² later generalized the method in such a way that nonadiabatic transitions can occur at any point in configuration space. At the same time, an algorithm — the so-called fewest switches criterion — was proposed which minimizes the number of surface hops per trajectory whilst guaranteeing the correct ensemble averaged state populations at all times. The latter is important because excessive surface switching effectively results in weighted averaging over the adiabatic states much like in the case of the Ehrenfest method.

We shall now derive the fewest switches criterion. Out of a total of N trajectories, N_k will be in state Ψ_k at time t ,

$$N_k(t) = \rho_{kk}(t)N \quad (84)$$

where we have introduced the density matrix notation

$$\rho_{kl}(t) = a_k^*(t)a_l(t). \quad (85)$$

At a later time $t' = t + \delta t$, the new occupation numbers are

$$N_k(t') = \rho_{kk}(t')N. \quad (86)$$

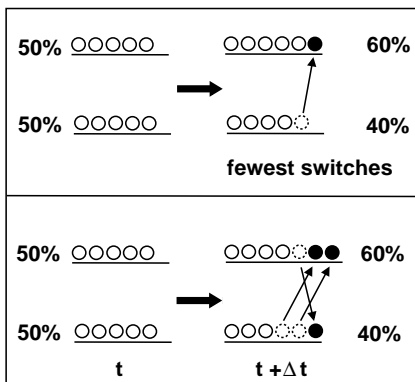


Fig. 7. A two-state system with each state being equally (50%) populated at time t . At time $t + \Delta t$ the lower and the upper state are populated by 40% and 60% of ensemble members, respectively. The top panel shows how this distribution can be achieved with the minimum number of transitions, whereas the bottom panel shows *one* alternative route involving a larger number of transitions.

Let us suppose that $N_k(t') < N_k(t)$ or $\delta N_k = N_k(t) - N_k(t') > 0$. Then the minimum number of transitions required to go from $N_k(t)$ to $N_k(t')$ is δN_k hops from state Ψ_k to any other state and zero hops from any other state to state Ψ_k , see Fig. 7. The probability $P_k(t, \delta t)$ for a transition out of state Ψ_k to any other state during the time interval $[t, t + \delta t]$ is then given by

$$P_k(t, \delta t) = \frac{\delta N_k}{N_k} = \frac{\rho_{kk}(t) - \rho_{kk}(t')}{\rho_{kk}} \approx -\frac{\dot{\rho}_{kk} \delta t}{\rho_{kk}} \quad (87)$$

where we have used

$$\dot{\rho}_{kk} \approx \frac{\rho_{kk}(t') - \rho_{kk}(t)}{\delta t}. \quad (88)$$

The left hand side of (88) can be written as

$$\begin{aligned} \dot{\rho}_{kk} &= \frac{d}{dt}(a_k^* a_k) = \dot{a}_k^* a_k + a_k^* \dot{a}_k \\ &= (a_k^* \dot{a}_k)^* + a_k^* \dot{a}_k = 2\Re(a_k^* \dot{a}_k) \end{aligned} \quad (89)$$

and inserting (64) into (89), we obtain

$$\dot{\rho}_{kk} = -2\Re \left(\sum_l \rho_{kl} C_{kl} e^{-\frac{i}{\hbar} \int (E_l - E_k) dt} \right). \quad (90)$$

Substituting expression (90) into (87), the probability P_k can be rewritten as follows

$$P_k(t, \delta t) = \frac{2\Re \left(\sum_l \rho_{kl} C_{kl} e^{-\frac{i}{\hbar} \int (E_l - E_k) dt} \right) \delta t}{\rho_{kk}}. \quad (91)$$

Since the probability, P_k , for a switch from state Ψ_k to any other state must be the sum over all states of the probabilities, P_{kl} , for a transition from state Ψ_k to a specific state Ψ_l

$$P_k(t, \delta t) = \sum_l P_{kl}(t, \delta t) \quad (92)$$

it follows from (91) that

$$P_{kl}(t, \delta t) = \frac{2\Re \left(\rho_{kl} C_{kl} e^{-\frac{i}{\hbar} \int (E_l - E_k) dt} \right) \delta t}{\rho_{kk}}. \quad (93)$$

A transition from state Ψ_k to state Ψ_m is now invoked if

$$P_k^{(m-1)} < \zeta < P_k^{(m)} \quad (94)$$

where ζ ($0 \leq \zeta \leq 1$) is a uniform random number and $P_k^{(m)}$ is the sum of the transition probabilities for the first m states,

$$P_k^{(m)} = \sum_l^m P_{kl}. \quad (95)$$

In order to conserve total energy after a surface hop has been carried out, the atomic velocities have to be rescaled. The usual procedure^{142,155} is to adjust only the velocity components in the direction of the nonadiabatic coupling vector $\mathbf{d}_{km}(\mathbf{R})$, see (77). We can qualitatively justify this practice by our earlier observation that the nonadiabatic contribution to the Ehrenfest forces also are in the direction of the nonadiabatic coupling vector $\mathbf{d}_{km}(\mathbf{R})$, see (83). Certainly, such discontinuities in nuclear velocities must be regarded as a flaw of the surface hopping approach. In most physical scenarios, however, non-adiabatic surface switches take place only at relatively small potential energy separations so that the necessary adjustment to the nuclear velocities is reasonably small. Nevertheless, a severe limitation of the method is presented by its inability to properly deal with situations in which the amount of kinetic energy is insufficient to compensate for the difference in potential energy (so-called classically forbidden transitions). Tully's original suggestion not to carry out a surface hop while retaining the nuclear velocities

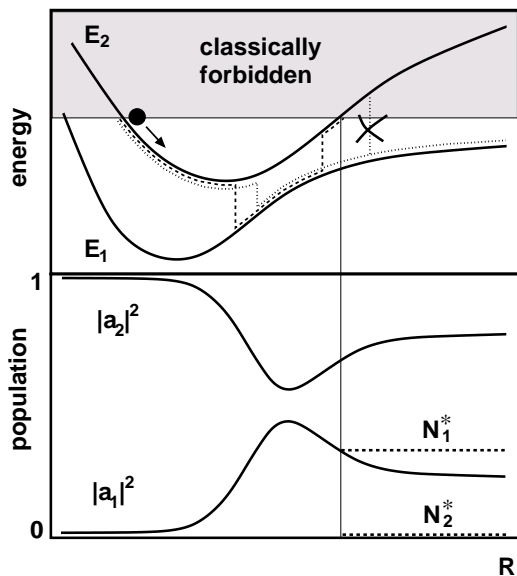


Fig. 8. Top: avoided crossing between two adiabatic potential energy surfaces, E_1 and E_2 , and two typical forward surface hopping trajectories. Nonadiabatic transitions are most likely to occur in the coupling region. The cross indicates a classically forbidden transition; no switch is carried out in this case. Bottom: corresponding adiabatic state populations $|a_1|^2$ and $|a_2|^2$. The system is prepared in state Ψ_2 initially with zero kinetic energy. Upon entering the coupling region state Ψ_1 is increasingly populated. Upon exiting the coupling region, the state population of Ψ_1 decreases. For configurations \mathbf{R} for which E_2 is in the classically forbidden region, the percentages of trajectories in state Ψ_k , N_k^* , are unequal to $|a_k|^2$; N_2^* is zero whereas N_1^* remains constant.

in such cases has been demonstrated¹⁵⁶ to be more accurate than later proposals^{155,157} to reverse the velocity components in the direction of the non-adiabatic coupling vector $\mathbf{d}_{km}(\mathbf{R})$. The example presented in Fig. 8 illuminates how classically forbidden transitions cause divergence between the target occupation numbers, $|a_k|^2$, and the actual percentages of trajectories evolving in state k , N_k^* .

Like the Ehrenfest method, surface hopping in the formulation presented here does not satisfy microscopic reversibility. This means that transition state theory for treating rare events cannot be applied rigorously,¹⁵⁸ since half-trajectories have to be integrated forward and backward in time starting at the transition state.

In contrast to the Ehrenfest approach, however, surface hopping is not representation-independent; it

has been demonstrated¹⁴⁵ that the adiabatic representation chosen here is best suited for surface hopping simulations.

It should be noted that surface hopping exhibits a large degree of electronic coherence through continuous integration of (64) along the entire trajectory. On the one hand, this enables the method to reproduce quantum interference effects¹⁴² such as Stückelberg oscillations.¹³⁹ On the other hand, due to treating nuclei classically, dephasing of the electronic degrees of freedom may be too slow, a shortcoming shared by the surface hopping and the Ehrenfest method alike. A number of semiclassical approaches incorporating decoherence have, therefore, been proposed.^{159–165} To some extent, recurrences are suppressed naturally, however, with increasing number of degrees of freedom (for example in condensed phases). This has been demonstrated even for rather small molecules in the gas phase.^{35,166,167}

Some of these alternative methods attempt to combine the advantages of surface hopping (mainly, pure adiabatic states in asymptotic regions) with those of the mean-field method (no discontinuities in potential energy, no disallowed transitions) by employing an effective potential whilst enforcing gradual demixing of the total wavefunction away from the coupling regions.^{163–165} Comparisons of surface hopping with other, very different methods can be found in the literature, e.g. Refs. 168 and 169.

4.1.4. Towards exact quantum dynamics

The methods discussed so far assume that the nuclei can be treated as classical point particles so that straightforward classical molecular dynamics techniques can be used in order to propagate them. It is certainly desirable to go beyond this approximation, in particular since nonadiabatic transitions are genuine quantum-mechanical events that call, in principle, for a quantum treatment of the nuclei as well. It is clear that a straightforward implementation of propagating the *total* Schrödinger Eqs. (1) and (2) is not possible except for *very* small systems due to the exponential complexity of the problem; see for instance, Ref. 170 for a recent study of an HD molecule subject of a strong laser pulse. Many systematic approaches to a coupled quantum dynamics of electrons and nuclei can be derived by using

a time-dependent (Dirac, Frenkel, McLachlan etc.) variational principle^{171–173} in conjunction with an (certain restricted) ansatz for the wavefunction (which is often represented by Gaussian wavepackets¹⁷⁴) in order to derive suitable equations of motion. For instance, the so-called “electron-nuclear dynamics” (END) method and its extensions are mainly used in order to study scattering processes involving a few atoms or small molecules.^{17,175} The so-called “fermionic molecular dynamics” (FMD) method was developed in order to cope with the antisymmetry of fermions in general, but it was mostly applied in the framework of nuclear physics.¹⁷⁶

A very powerful algorithm to propagate wavepackets for nuclei is the multiconfiguration time-dependent Hartree (MCTDH) method.^{177,178} Currently this approach is used to treat of the order of 10–100 coupled nuclear degrees of freedom — including several electronic states! However, it is required that the Hamiltonian can be expanded as a sum of products of one-particle operators, which implies that the interaction potential has to be transformed according to this constraint. In view of this prerequisite is seems difficult to compute the interactions “on the fly” as the nuclei are propagated, so that the bottleneck is the availability of potential energy surfaces in 10–100 dimensions.

Finally, a promising approach to both large systems and nonadiabatic dynamics is the so-called “full multiple spawning method” (FMS) in its *ab initio* extension (AIMS); see Ref. 179 for a review article. It relies on expanding the nuclear wavefunction in terms of Gaussian wavepackets, with the possibility of increasing their number as needed, together with the evaluation of energies, gradients and nonadiabatic couplings not in advance, but as the Gaussians move in time. This idea will be presented in more detail in Sec. 4.2.5.

4.2. First principles implementation of nonadiabatic dynamics

4.2.1. Wavefunction-based methods

A nonadiabatic *ab initio* molecular dynamics approach based on an approximate Hartree–Fock scheme using the fewest-switches surface hopping

algorithm¹⁴² to couple the first excited state to the ground state was introduced recently.¹⁸⁰ The notion “*ab initio* Wigner distribution approach to nonadiabatic dynamics” was coined in Ref. 180 since a Wigner expansion was used for the vibronic density matrix in order to establish the canonical ensemble. The calculation of electronic structure and in particular the evaluation of the nonadiabatic couplings is performed in the so-called “frozen ionic bonds” approximation.⁹⁷ This simplification implies that the only allowed electronic excitations are those that arise from promoting an unpaired electron in the HOMO of the molecule while keeping the underlying doubly occupied orbitals frozen. In addition, effective core potentials or pseudo potentials were used in order to reduce the number of active electronic degrees of freedom. Using this method the evaluation of both gradients and couplings is considerably less demanding as compared to using other suitable approaches such as RPA, CASSCF, or CI without sacrificing too much accuracy because of the favorable energy-level structure underlying the “frozen ionic bonds” scheme.

The time-dependent electronic wavefunction is expanded in terms of an adiabatic basis set

$$\Psi(\mathbf{r}; t) = \sum_l a_l(t) \Psi_l(\mathbf{r}, \mathbf{R}) \quad (96)$$

stemming from the *one-electron* Hamiltonian in the “frozen ionic bonds” formulation at the instantaneous configuration $\mathbf{R}(t)$ of the nuclei. This leads to the usual Schrödinger equations

$$i\dot{a}_k(t) = \epsilon_k a_k(t) - i \sum_{lI} \dot{\mathbf{R}}_I \mathbf{d}_{kl}^I a_l(t) \quad (97)$$

$$\mathbf{d}_{kl}^I = \langle \Psi_k | \nabla_I | \Psi_l \rangle \quad (98)$$

for the time-dependent expansion coefficients in this particular orthogonal basis (atomic units are used throughout this subsection). An analytical expression of an explicit evaluation of the nonadiabatic coupling vectors \mathbf{d}_{kl}^I is derived in Ref. 180 within the “frozen ionic bonds” approximation. The corresponding Newtonian equations of motion for the classical nuclei moving in the k th electronic state are given by

$$M_I \ddot{\mathbf{R}}_I = -\nabla_I (E^{\text{cHF}}(\mathbf{R}) - \epsilon_0(\mathbf{R}) + \epsilon_k(\mathbf{R})) \quad (99)$$

where E^{cHF} and ϵ_0/ϵ_k denote the SCF energy of the frozen ionic core and the eigenvalues of the single electron in the field of the core, respectively, see Ref. 97. Together with the fewest-switches hopping probability, see (87),

$$P_{kl} = \frac{2\delta t}{|a_k|^2} \left(\Im[a_k^* a_l \epsilon_k \delta_{kl}] - \Re \left[a_k^* a_l \sum_I \dot{\mathbf{R}}_I \mathbf{d}_{kl}^I \right] \right) \quad (100)$$

this completes the presented approach to performing nonadiabatic molecular dynamics “on the fly”.

This method was used in order to study in great detail the femtosecond photoisomerization process due to a radiationless decay from the first excited state through a conical intersection in a five-atom cluster.¹⁸⁰

An important contribution to the *ab initio* exploration of excited state potential energy surfaces has been made by applying quantum chemistry methods in order to characterize conical intersection funnels.³⁸ For a variety of organic molecules, the decay paths from the excited state to the ground state via a conical intersection^{33,36,37} have been determined by computing the minimum energy path (MEP)¹⁸¹ using the intrinsic reaction coordinate (IRC) method.¹⁸² Such an approach, however, does not provide a full *dynamical* picture in the sense of proper evolution in real time, since the atomic nuclei have infinitesimal kinetic energy.

The photoisomerization dynamics of a retinal chromophore model has recently been described using a CASSCF based surface hopping approach.¹⁸³

4.2.2. Time-dependent density functional theory in the time domain

In principle, time-dependent density functional theory^{71,124–126} can be used in order to describe the fully coupled time evolution of quantum systems. Presently, this theory and in particular its linear response formulation is extensively used for the calculation of excited state energies, optical spectra, hyperpolarizabilities etc. given a set of *space-fixed* classical nuclei. Most often, it is used in the frequency domain since there the poles of the linear density response directly yield the excitation energies.¹²⁸

Compared to such studies only few implementations of a propagation of these equations directly in real time exist. However, most of the approaches within this class are restricted to adiabatic time evolution which is justified in many situations, see for instance, Refs. 183–189.

A notable exception is the explicit real-time formulation of a nonadiabatic quantum molecular dynamics scheme based on time-dependent Kohn–Sham theory.^{190,191} As usual for such approaches, the first step consists in separating the classical nuclear degrees of freedom from the electronic ones according to (16). In a second step, a coupled set of equations of motion for nuclei and electrons are obtained from requiring that the total energy is conserved. The electronic subsystem is described within time-dependent density functional theory (atomic units are used throughout this subsection)

$$i \frac{\partial \psi_i(\mathbf{r}; t)}{\partial t} = \left[-\frac{1}{2} \nabla^2 + V^{\text{KS}} \right] \psi_i(\mathbf{r}; t) \quad (101)$$

where ψ_i are the occupied time-dependent Kohn–Sham orbitals, n is the corresponding density

$$n(\mathbf{r}; t) = \sum_j^{\text{occ}} |\psi_j(\mathbf{r}; t)|^2 \quad (102)$$

and V^{KS} is the Kohn–Sham potential

$$V^{\text{KS}} = - \sum_I \frac{Z_I}{|\mathbf{r} - \mathbf{R}_I|} + V_{\text{H}} + V_{\text{xc}} \quad (103)$$

with $V_{\text{H}} = \int d\mathbf{r}' n(\mathbf{r}')/|\mathbf{r} - \mathbf{r}'|$ denoting the Hartree potential and V_{xc} denoting the (true) time-dependent exchange-correlation potential; see for instance, Ref. 71 for more details. Being a one-determinantal single-particle representation of the total density, the Kohn–Sham orbitals can be expanded in terms of an arbitrary single-particle basis

$$\psi_i(\mathbf{r}; t) = \sum_{\alpha} a_{\alpha i}(t) \phi_{\alpha}(\mathbf{r}, \mathbf{R}) \quad (104)$$

that depends parametrically on the time-dependent nuclear positions $\mathbf{R}(t)$. This leads to the following formulation of the time-dependent Kohn–Sham equations

$$i \dot{a}_{\alpha i}(t) = \sum_{\beta\gamma} (S^{-1})_{\alpha\beta} \left\{ H_{\beta\gamma} - i \sum_I \dot{\mathbf{R}}_I \mathbf{d}_{\beta\gamma}^I \right\} a_{\gamma i}(t) \quad (105)$$

with the nonadiabatic coupling vector matrix

$$\mathbf{d}_{\alpha\beta}^I = \langle \phi_\alpha | \nabla_I | \phi_\beta \rangle \quad (106)$$

the overlap matrix

$$S_{\alpha\beta} = \langle \phi_\alpha | \phi_\beta \rangle \quad (107)$$

and the Hamiltonian matrix

$$H_{\alpha\beta} = \left\langle \phi_\alpha \left| -\frac{1}{2} \nabla^2 + V^{\text{KS}} \right| \phi_\beta \right\rangle. \quad (108)$$

The corresponding equations of motion for the classical nuclei can be written as

$$M_I \ddot{\mathbf{R}}_I = -\nabla_I \sum_J \frac{Z_I Z_J}{|\mathbf{R}_I - \mathbf{R}_J|} - \sum_j \left\{ \sum_{\alpha\beta} a_{\alpha j}^* [\nabla_I H_{\alpha\beta} - \langle \phi_\alpha | \nabla_I (V_{\text{H}} + V_{\text{xc}}) | \phi_\beta \rangle] a_{\beta j} - \sum_{\alpha\beta\gamma\delta} a_{\alpha j}^* [H_{\alpha\beta} (S^{-1})_{\beta\gamma}] \mathbf{d}_{\gamma\delta}^I + (\mathbf{d}^T)_{\alpha\beta}^I (S^{-1})_{\beta\gamma} H_{\gamma\delta}] a_{\delta j} \right\} \quad (109)$$

in terms of the various matrix elements introduced above. The coupled set of electronic and nuclear equations of motion (105) and (109) define what could be called Ehrenfest molecular dynamics based on time-dependent Kohn–Sham density functional theory (note that the more general notion “non-adiabatic quantum molecular dynamics” or NA–QMD was coined in Ref. 190). It can be shown that in the absence of electronic transitions these equations reduce to the well-known adiabatic equations with trivial stationary-state time evolution.^{190,191} It should be noted that electronic excitations are achieved via coupling to external perturbation, such as for example an external electromagnetic field which in general, does not produce a dynamical evolution starting in a particular preselected pure state.

Using the collision of a proton with a hydrogen atom as an example this approach was used in Refs. 190 and 191 to demonstrate the effects of nonadiabatic transitions on the motion of the nuclei within the above framework. Shortly later, this approach was applied to complex many-body atom/cluster and ion/fullerene collision processes.^{192–195} A formulation including an external laser field was given most recently.¹⁹⁶ A very similar approach was developed in Ref. 197 and applied to investigate the laser-response of C₆₀ and carbon chains within an approximate (tight-binding) density functional scheme.¹⁹⁸

4.2.3. Car–Parrinello surface hopping

In the case of ground state calculations, density functional theory^{70–73} based *ab initio* molecular dynamics

simulations in the spirit of Car and Parrinello¹⁰ have become the method of choice to study large molecules and condensed phase systems (see Sec. 2.2). As we have discussed in Sec. 3.3, Car–Parrinello simulations have become possible also in the first excited state using a restricted open-shell Kohn–Sham (ROKS) approach.¹¹⁰ A nonadiabatic extension of the Car–Parrinello method coupling the ROKS S_1 excited state to the S_0 ground state using a Tully-style¹⁴² trajectory surface hopping algorithm has been presented in Ref. 118 and will be outlined in this subsection, see also Ref. 148.

As we have shown in Sec. 3.3, the S_1 restricted open-shell singlet wavefunction is constructed by linearly combining the mixed determinants, m_1 and m_2 (see Fig. 1),

$$\begin{aligned} \Psi_1 &= \frac{1}{\sqrt{2}} \{ |m_1\rangle + |m_2\rangle \} \\ &= \frac{1}{\sqrt{2}} \{ |\psi_1^{(1)} \bar{\psi}_1^{(1)} \psi_2^{(1)} \bar{\psi}_2^{(1)} \dots \psi_l^{(1)} \bar{\psi}_{l+1}^{(1)} \rangle \\ &\quad + |\psi_1^{(1)} \bar{\psi}_1^{(1)} \psi_2^{(1)} \bar{\psi}_2^{(1)} \dots \bar{\psi}_l^{(1)} \psi_{l+1}^{(1)} \rangle \} \quad (110) \end{aligned}$$

where the “ket” notation signifies Slater determinants made up of Kohn–Sham orbitals, $\psi_i^{(1)}$ (spin up) and $\bar{\psi}_i^{(1)}$ (spin down); $l = n/2$ is half the number of electrons.

We recall (Sec. 3.3) that the S_1 energy, $E(S_1)$, can be written as the difference between twice the energy of the mixed determinant, $E(m)$, and the energy of the triplet determinant, $E(t)$,

$$E(S_1) = 2E(m) - E(t). \quad (111)$$

Within the ROKS scheme, a *single* set of orbitals $\{\psi_i^{(1)}\}$ is determined that minimizes the energy functional

$$E[\{\psi_i^{(1)}\}] = 2\langle m|\mathcal{H}^{\text{KS}}|m\rangle - \langle t|\mathcal{H}^{\text{KS}}|t\rangle - \sum_{i,j=1}^{l+1} \lambda_{ij} \{\langle \psi_i^{(1)}|\psi_j^{(1)}\rangle - \delta_{ij}\} \quad (112)$$

where \mathcal{H}^{KS} is the Kohn–Sham Hamiltonian⁷³ and the λ_{ij} are Lagrange multipliers taking care of the orthonormality of the orbitals. Due to this optimization the entire set of orbitals $\{\psi_i^{(1)}\}$ will, in general, differ from the set of orbitals $\{\psi_i^{(0)}\}$ that define the ground state wavefunction, Ψ_0 ,

$$\Psi_0 = |\psi_1^{(0)}\bar{\psi}_1^{(0)}\psi_2^{(0)}\bar{\psi}_2^{(0)}\dots\psi_l^{(0)}\bar{\psi}_l^{(0)}\rangle. \quad (113)$$

As a consequence the two state functions, Ψ_0 and Ψ_1 , are nonorthogonal giving rise to the overlap matrix elements, S_{kl} ,

$$S_{01} = S_{10} \equiv S, \quad S_{kk} = 1. \quad (114)$$

Inserting ansatz (63) using the above basis functions, Ψ_0 and Ψ_1 , into (62) and replacing \mathcal{H}_{e1} with \mathcal{H}^{KS} we obtain after integration over the electronic coordinates following multiplication by Ψ_k^* from the left

$$\sum_l a_l p_l (H_{kl} - E_l S_{kl}) = i\hbar \left\{ \sum_l \dot{a}_l p_l S_{kl} + \sum_l a_l p_l C_{kl} \right\} \quad (115)$$

where the Hamiltonian matrix elements are given by

$$H_{kk} = \langle \Psi_k|\mathcal{H}^{\text{KS}}|\Psi_k\rangle = E_k \quad (116)$$

$$H_{01} = H_{10} = E_0 S \quad (117)$$

and the phase factor has been abbreviated as

$$p_l \equiv e^{-\frac{i}{\hbar} \int E_l dt}. \quad (118)$$

For $k = 0$, (115) becomes

$$a_1 p_1 S (E_0 - E_1) = i\hbar \{ \dot{a}_0 p_0 + \dot{a}_1 p_1 S + a_1 p_1 C_{01} \} \quad (119)$$

and for $k = 1$

$$0 = \dot{a}_0 p_0 S + \dot{a}_1 p_1 + a_0 p_0 C_{10}. \quad (120)$$

We should stress here that the discrepancy between (115) and (64) arises purely because Ψ_1 is *not* an eigenfunction of \mathcal{H}^{KS} . In the limit $S = 0$, however, we recover (64).

Solving Eqs. (119) and (120) for \dot{a}_0 and \dot{a}_1 one finds

$$\dot{a}_0 = \frac{1}{S^2 - 1} \left[ia_1 \frac{p_1}{p_0} S (E_0 - E_1) + a_1 C_{01} \frac{p_1}{p_0} - a_0 C_{10} S \right] \quad (121)$$

$$\dot{a}_1 = \frac{1}{S^2 - 1} \left[a_0 C_{10} \frac{p_0}{p_1} - a_1 C_{01} S - ia_1 S^2 (E_0 - E_1) \right]. \quad (122)$$

We integrate these two coupled differential equations numerically using a fourth order Runge–Kutta scheme.¹⁹⁹ It is computationally attractive to work with the nonadiabatic coupling elements, C_{kl} , see (65), instead of the nonadiabatic coupling vectors, \mathbf{d}_{lk} , see (77), since the orbital velocities are readily available within the Car–Parrinello method. A Born–Oppenheimer implementation is also possible, in which case the nonadiabatic couplings have to be computed using a finite difference scheme.

If both electronic state functions were eigenfunctions of the Kohn–Sham Hamiltonian, $|a_0|^2$ and $|a_1|^2$

would be their respective occupation numbers. A look at the normalization integral of the total wavefunction, Ψ ,

$$\langle \Psi|\Psi\rangle = |a_0|^2 + |a_1|^2 + 2S \Re \left(a_0^* a_1 \frac{p_1}{p_0} \right) \equiv 1 \quad (123)$$

shows that the definition of state populations in this basis is ambiguous. We therefore expand the total wavefunction Ψ in terms of an orthonormal set of auxiliary wavefunctions, Ψ'_0 and Ψ'_1

$$\Psi = d_0 \Psi'_0 + d_1 \Psi'_1 = b_0 \Psi_0 + b_1 \Psi_1 \quad (124)$$

where

$$\langle \Psi'_k | \Psi'_l \rangle = \delta_{kl} \quad (125)$$

and

$$b_j = a_l p_l. \quad (126)$$

Since Ψ is normalized, the squares of our new expansion coefficients add up to unity and thus have the meaning of state populations in the orthogonal basis

$$|d_0|^2 + |d_1|^2 = 1. \quad (127)$$

The orthonormal wavefunctions Ψ'_0 and Ψ'_1 can be expressed in terms of Ψ_0 and Ψ_1 as

$$\Psi'_0 = c_{00}\Psi_0 + c_{10}\Psi_1 \quad (128)$$

$$\Psi'_1 = c_{01}\Psi_0 + c_{11}\Psi_1 \quad (129)$$

$\mathbf{c}_0 = \begin{pmatrix} c_{00} \\ c_{10} \end{pmatrix}$ and $\mathbf{c}_1 = \begin{pmatrix} c_{01} \\ c_{11} \end{pmatrix}$ being solutions of the eigenvalue problem

$$\mathbf{HC} = \mathbf{SCE}. \quad (130)$$

Using the Hamiltonian matrix elements of (116) and (117) and the overlap matrix of (114), one obtains the eigenvalues

$$e_0 = E_0 \quad (131)$$

and

$$e_1 = \frac{E_1 - S^2 E_0}{1 - S^2} \quad (> E_1, \text{ if } E_0 < E_1). \quad (132)$$

The corresponding eigenvectors are

$$\mathbf{c}_0 = \begin{pmatrix} 1 \\ 0 \end{pmatrix} \quad (133)$$

and

$$\mathbf{c}_1 = \begin{pmatrix} -S \\ 1 \end{pmatrix} \quad (134)$$

leading to the orthonormal wavefunctions

$$\Psi'_0 = \Psi_0 \quad (135)$$

$$\Psi'_1 = \frac{1}{\sqrt{1 - S^2}} [-S\Psi_0 + \Psi_1]. \quad (136)$$

Inserting (135) and (136) into (124), we determine the expansion coefficients to be

$$d_0 = b_0 + b_1 S \quad (137)$$

$$d_1 = b_1 \sqrt{1 - S^2}. \quad (138)$$

The state occupation numbers are thus

$$|d_0|^2 = |b_0|^2 + S^2 |b_1|^2 + 2S \Re(b_0^* b_1) \quad (139)$$

$$|d_1|^2 = (1 - S^2) |b_1|^2 \quad (140)$$

or alternatively

$$|d_0|^2 = |a_0|^2 + S^2 |a_1|^2 + 2S \Re\left(a_0^* a_1 \frac{p_1}{p_0}\right) \quad (141)$$

$$|d_1|^2 = (1 - S^2) |a_1|^2. \quad (142)$$

We are now in a position to apply Tully's fewest switches criterion (93) using the coefficients d_k to construct the density matrix (85).

For many applications the overlap S is sufficiently small so that nuclear gradients may be obtained from the uncorrected excited state energy, E_1 . In the case of formaldehyde,¹¹⁸ $S^2 = 4.9 \times 10^{-3}$ for ground state optimized geometry — corresponding to a correction to the S_1 energy of 0.02 eV according to (132) — and $S^2 = 1.3 \times 10^{-4}$ for S_1 optimized geometry.

4.2.4. Incoherent thermal excitations via free energy functionals

The free energy functional or ensemble density functional theory approaches to excited-state molecular dynamics^{200–202} are mean-field approaches that are similar in spirit to Ehrenfest molecular dynamics, see Sec. 4.1.2. The total wavefunction is first factorized into a nuclear and an electronic wavefunction (16) followed by taking the classical limit for the nuclear subsystem, see Sec. 2.1.2. Thus, classical nuclei move in the *average* field as obtained from appropriately weighting all electronic states similar to (72). A difference is that according to Ehrenfest molecular dynamics the electrons are propagated in real time and can perform nonadiabatic transitions by virtue of direct coupling terms $\propto \mathbf{d}_{kl}$ between all states Ψ_k subject to energy conservation, see Sec. 4.1.2. The average force or Ehrenfest force (83) is obtained by weighting the different states k according to their diagonal density matrix elements, that is $\propto |a_k(t)|^2$. In addition, *coherent* transitions between the excited states are driven by the off-diagonal contributions to the density matrix which are given by $a_k^* a_l$ in (83).

In the free energy ensemble approaches,^{200–202} the excited states are populated instead according to

the Fermi–Dirac finite-temperature equilibrium distribution. This is based on the assumption that the electrons always “equilibrate” instantaneously given a new nuclear configuration, i.e. the electrons move very rapidly on the timescale of the nuclear motion. This means that the set of electronic states evolves at a given temperature “isothermally” (rather than adiabatically) under the inclusion of *incoherent* electronic transitions as the nuclei move. Thus, instead of computing the force acting on the nuclei from some state-averaged energy (72) it is obtained from the electronic *free* energy as defined in the canonical ensemble at a certain nonzero temperature. By allowing the population of excited electronic states including changes of these populations to occur, the free energy approach clearly goes beyond the usual Born–Oppenheimer and adiabatic approximations. However, the approximation of an instantaneous (thermal) equilibration of the electronic subsystem implies that the electronic structure at a given nuclear configuration $\mathbf{R}(t)$ is completely independent from previous configurations $\mathbf{R}(t')$ along a molecular dynamics trajectory. This type of nonadiabaticity clearly is *very different* from other nonadiabatic molecular dynamics methods such as the ones by Ehrenfest and Tully, see Secs. 4.1.2 and 4.1.3, respectively. Due to the underlying assumption of still using a product ansatz (16) the notion “free energy Born–Oppenheimer approximation” was coined in Ref. 203 in a similar context. Within this philosophy certain nonequilibrium situations can also be modeled within the free energy approach. This can be achieved by starting off with an initial orbital occupation pattern that does not correspond to any temperature in its thermodynamic meaning, see for example Refs. 204–207 for such applications.

The particular free energy functional as introduced in Ref. 200 is derived most elegantly^{201,208} by starting the discussion for the special case of *noninteracting* fermions (atomic units are used throughout this subsection)

$$\mathcal{H}_s = -\frac{1}{2}\nabla^2 - \sum_I \frac{Z_I}{|\mathbf{R}_I - \mathbf{r}|} \quad (143)$$

in a *fixed* external potential due to a collection of nuclei at positions \mathbf{R} . The associated grand partition function and its thermodynamic potential (“grand free energy”) are given by

$$\Xi_s(\mu VT) = \det^2(1 + \exp[-\beta(\mathcal{H}_s - \mu)]) \quad (144)$$

$$\Omega_s(\mu VT) = -k_B T \ln \Xi_s(\mu VT) \quad (145)$$

respectively, where μ is the chemical potential acting on the electrons and the square of the determinant stems from considering the spin-unpolarized special case only; $\beta = 1/k_B T$ as usual. This reduces to the well-known grand potential expression

$$\begin{aligned} \Omega_s(\mu VT) &= -2k_B T \ln \det(1 + \exp[-\beta(\mathcal{H}_s - \mu)]) \\ &= -2k_B T \sum_i \ln(1 + \exp[-\beta(\epsilon_i^s - \mu)]) \end{aligned} \quad (146)$$

for noninteracting spin- $\frac{1}{2}$ fermions where $\{\epsilon_i^s\}$ are the eigenvalues of a one-particle Hamiltonian such as (143); here the standard identity $\ln \det \mathcal{M} = \text{Tr} \ln \mathbf{M}$ was invoked for positive definite operator \mathcal{M} and its matrix representation \mathbf{M} .

According to standard thermodynamics the Helmholtz free energy $\mathcal{F}(NVT)$ associated to (145) can be obtained from an appropriate Legendre transformation of the grand free energy $\Omega(\mu VT)$

$$\mathcal{F}_s(NVT) = \Omega_s(\mu VT) + \mu N + \sum_{I < J} \frac{Z_I Z_J}{|\mathbf{R}_I - \mathbf{R}_J|} \quad (147)$$

by fixing the average number of electrons N and determining μ from the conventional thermodynamic condition

$$N = - \left(\frac{\partial \Omega}{\partial \mu} \right)_{VT}. \quad (148)$$

In addition, the internuclear Coulomb interactions between the classical nuclei were included at this stage in (147). Thus, derivatives of the free energy (147) with respect to ionic positions $-\nabla_I \mathcal{F}_s$ define forces on the nuclei that could be used in a (hypothetical) molecular dynamics scheme using noninteracting electrons.

The interactions between the electrons can be “switched on” by resorting to Kohn–Sham density functional theory and the concept of a noninteracting reference system. Thus, instead of using the simple one-particle Hamiltonian (143), the Kohn–Sham Hamiltonian^{70,71} has to be utilized. As a result, the grand free energy (144) can be written as

$$\Omega^{\text{KS}}(\mu VT) = -2k_{\text{B}}T \ln[\det(1 + \exp[-\beta(\mathcal{H}^{\text{KS}} - \mu)])] \quad (149)$$

$$\mathcal{H}^{\text{KS}} = -\frac{1}{2}\nabla^2 - \sum_I \frac{Z_I}{|\mathbf{R}_I - \mathbf{r}|} + V_{\text{H}}(\mathbf{r}) + \frac{\delta\Omega_{\text{xc}}[n]}{\delta n(\mathbf{r})} \quad (150)$$

$$\mathcal{H}^{\text{KS}}\psi_i = \epsilon_i\psi_i \quad (151)$$

where Ω_{xc} is the exchange-correlation functional at finite temperature. By virtue of (146) one can immediately see that Ω^{KS} is nothing else than the “Fermi–Dirac weighted sum” of the bare Kohn–Sham eigenvalues $\{\epsilon_i\}$. Whence, this term is the extension to finite temperatures of the so-called “band-structure energy” (or of the “sum of orbital energies” in the analogous Hartree–Fock case^{209,210}) contribution to the total electronic energy.

In order to obtain the correct total electronic free energy of the *interacting* electrons the corresponding extra terms (properly generalized to finite temperatures) have to be included in Ω^{KS} . This finally allows one to write down the generalization of the Helmholtz free energy of the interacting many-electron case

$$\begin{aligned} \mathcal{F}^{\text{KS}}(NVT) &= \Omega^{\text{KS}}(\mu VT) + \mu \int d\mathbf{r} n(\mathbf{r}) \\ &+ \sum_{I < J} \frac{Z_I Z_J}{|\mathbf{R}_I - \mathbf{R}_J|} - \frac{1}{2} \int d\mathbf{r} V_{\text{H}}(\mathbf{r}) n(\mathbf{r}) \\ &+ \Omega_{\text{xc}} - \int d\mathbf{r} \frac{\delta\Omega_{\text{xc}}[n]}{\delta n(\mathbf{r})} n(\mathbf{r}) \end{aligned} \quad (152)$$

in the framework of a Kohn–Sham-like formulation. The corresponding one-particle density at the Γ -point is given by

$$n(\mathbf{r}) = \sum_i f_i |\psi_i(\mathbf{r})|^2 \quad (153)$$

$$f_i = (1 + \exp[\beta(\epsilon_i - \mu)])^{-1} \quad (154)$$

where the fractional occupation numbers $\{f_i\}$ are obtained from the Fermi–Dirac distribution at temperature T in terms of the Kohn–Sham eigenvalues $\{\epsilon_i\}$.

By construction, the total free energy (152) reduces to that of the noninteracting toy model (147) once the electron–electron interaction is switched off. Another useful limit is the ground-state limit $\beta \rightarrow \infty$

where the free energy $\mathcal{F}^{\text{KS}}(NVT)$ yields the standard Kohn–Sham total energy expression E^{KS} (see for instance Refs. 70 and 71) after invoking the appropriate limit $\Omega_{\text{xc}} \rightarrow E_{\text{xc}}$ as $T \rightarrow 0$. Most importantly, stability analysis^{200,201} of (152) shows that this functional shares the same stationary point as the exact finite-temperature functional due to Mermin,²¹¹ see for example the monographs Refs. 70 and 71 for introductions to density functional formalisms at finite temperatures. This implies that the self-consistent density, which defines the stationary point of \mathcal{F}^{KS} , is identical to the exact one. This analysis reveals furthermore that, unfortunately, this stationary point is not an extremum but a saddle point so that no variational principle and, numerically speaking, no direct minimization algorithms can be applied. For the same reason a Car–Parrinello fictitious dynamics approach to molecular dynamics is not a straightforward option, whereas Born–Oppenheimer dynamics based on diagonalization can be used directly. Thus, an iterative molecular dynamics scheme

$$M_I \ddot{\mathbf{R}}_I = -\nabla_I \mathcal{F}^{\text{KS}}(\mathbf{R}) \quad (155)$$

is introduced by computing the *ab initio* forces from the nuclear gradient of the free energy functional \mathcal{F}^{KS} taking advantage of the Hellmann–Feynman theorem.

As a method, molecular dynamics with the free energy functional is most appropriate to use when the electronic excitation gap is either small or when the gap might close during a chemical transformation. In the latter case no instabilities are encountered with this approach, which is not always true for ground-state *ab initio* molecular dynamics methods. The price to pay is the quite demanding iterative computation of well-converged forces. Besides allowing such applications with physically relevant excitations this method can also be straightforwardly combined with \mathbf{k} -point sampling and applied to metals at “zero” temperature. In this case, the electronic “temperature” is only used as a smearing parameter

of the Fermi edge by introducing fractional occupation numbers, which is known to improve greatly the convergence of these ground-state electronic structure calculations.^{60,202,212–219}

Finite-temperature expressions for the exchange-correlation functional Ω_{xc} are available in the literature. However, for most temperatures of interest the corrections to the ground-state expression are small and it seems justified to use one of the various well-established parameterizations of the exchange-correlation energy E_{xc} at zero temperature.^{70,71}

This particular approach to finite electronic temperature molecular dynamics has been used in order to investigate for instance the sound velocity of dense hydrogen at conditions on jupiter,²²⁰ laser heating of silicon^{204,205} and graphite,²⁰⁶ and laser-induced transformations in fullerite.²⁰⁷ In all cases the electronic subsystem was highly excited, either by imposing a very high equilibrium temperature for both (classical) nuclei and electrons,²²⁰ or by creating a pronounced nonequilibrium initial population of the excited electronic states in order to model the influence of an irradiating laser pulse.

An alternative variational formulation and implementation of ensemble density functional theory directly in the framework of the Mermin–Kohn–Sham approach starts by adopting a matrix representation of the Fermi operator

$$n(\mathbf{r}) = \sum_{ij} f_{ij} \psi_i^*(\mathbf{r}) \psi_j(\mathbf{r}) \quad (156)$$

in the basis of single-particle Kohn–Sham orbitals which yields a (fractional) occupation number matrix \mathbf{f} , see Ref. 202. In order to make this definition of occupation numbers meaningful the constraint $\text{Tr } \mathbf{f} = N$ that the trace of the occupation number matrix yields the total number of electrons in the system has to be imposed in addition to requiring that its eigenvalues are the usual occupation numbers, i.e. $f_i = \text{diag } \mathbf{f} \in [0, 1]$. The free energy functional \mathcal{A} to be minimized is defined as

$$\begin{aligned} \mathcal{A}[\psi, \mathbf{f}] = & \sum_{ij} f_{ij} \left\langle \psi_i \left| -\frac{1}{2} \nabla^2 - \sum_I \frac{Z_I}{|\mathbf{R}_I - \mathbf{r}|} \right| \psi_j \right\rangle \\ & + V_H[n] + V_{xc}[n] - T\mathcal{S}[\mathbf{f}] \end{aligned} \quad (157)$$

where the entropy term is given by

$$\mathcal{S}[\mathbf{f}] = -k_B \text{Tr} \{ \mathbf{f} \ln \mathbf{f} + (\mathbf{1} - \mathbf{f}) \ln (\mathbf{1} - \mathbf{f}) \}. \quad (158)$$

Now the free energy (157) obtained from traces of operators is covariant under both orbital and occupation number unitary transformations. This allows to introduce a new auxiliary functional

$$\tilde{\mathcal{A}}[\psi] = \min_{\{f_{ij}\}} \mathcal{A}[\psi, \mathbf{f}] \quad (159)$$

that is minimized wrt the occupation number matrix and thus depends only on the orbitals; it is also invariant under unitary transformations of the orbitals. This opens up the possibility of a two-step iterative minimization of \mathcal{A} by decoupling the orbital and occupation number evolution. In an outer loop the orbitals get updated by searching the minimum of $\tilde{\mathcal{A}}$, whereas the occupation number matrix gets updated by minimizing the corresponding functional \mathcal{A} while keeping the orbitals fixed; the orthogonality of the orbitals has to be imposed. The detailed algorithm that implements these ideas is discussed in Ref. 202.

This particular implementation of the Mermin–Kohn–Sham functional has been used to study the behavior of the Al(110) surface for temperatures up to 900 K via *ab initio* molecular dynamics.²²¹ Most recently, a full Car–Parrinello formulation in terms of a coupled fictitious dynamics of orbitals, occupation matrix, and unitary rotations was given as well as a hybrid scheme where the $\{f_{ij}\}$ get iteratively minimized during the fictitious time evolution of the orbitals.^{222,223}

The two methods presented so far both yield the correct ensemble density functional theory formulation for electronic systems at finite temperatures and thus require a self-consistent calculation of the occupation numbers. A similar but simplified approach to include finite electronic temperatures relies on total energy calculations where only the (fractional) occupation numbers of the Kohn–Sham single-particle states are chosen according to the Fermi–Dirac distribution for a certain temperature and chemical potential according to (154). Recently, such an ansatz was chosen in order to investigate the phonon response in photoexcited solid tellurium.²²⁴

All methods discussed so far allow for *thermal* excitations within Mermin’s version of ensemble density functional theory. In addition, it is also possible to create athermal initial distributions, which is however a slightly uncontrolled approach to generate electronic excitations. The intricacies of devising a density functional formulation for a particular excited state as

for instance defined by its symmetry within the framework of an ensemble Kohn–Sham scheme are discussed in Ref. 225. Unfortunately, this formulation relies crucially on the calculation of (nonlocal) optimized effective potentials (i.e. an orbital-dependent functional), which will prevent its use for *ab initio* molecular dynamics in the near future.

4.2.5. Traveling frozen Gaussians and multiple spawning

After having discussed several density-functional-based approaches to nonadiabatic molecular dynamics we finally discuss a promising approach that relies on ideas of both wavepacket dynamics and quantum chemistry. The so-called “full multiple spawning method” (FMS)^{226,227} is basically a nonadiabatic extension of wave packet dynamics based on frozen Gaussians.^{174,228–230} The latter can be defined for the one-dimensional case as

$$g(R; \bar{R}(t), \bar{P}(t), \bar{\gamma}(t), \alpha) = \left(\frac{2\alpha}{\pi}\right)^{1/4} \exp[-\alpha(R - \bar{R})^2 + i\bar{P}(R - \bar{R}) + i\bar{\gamma}] \quad (160)$$

where $\bar{R}(t)$, $\bar{P}(t)$, and $\bar{\gamma}(t)$ denote the explicitly time-dependent position, momentum and phase of each individual basis function. The width α of each Gaussian is fixed, i.e. it is treated as a time-independent parameter in any frozen Gaussian calculation according to which $(R - \bar{R}(t))^2$ describes harmonic quantum fluctuations with respect to the average position $\bar{R}(t)$ at time t . In its *ab initio* variant (dubbed AIMS)^{231–233} the potential energy surfaces and the nonadiabatic couplings between the different states are computed “on the fly” from concurrent electronic structure calculations, see Ref. 179 for a review article. Thus, at variance with most other methods presented in our review, the FMS/AIMS approach includes also quantum effects of the nuclei to some extent; an extension in order to treat nuclear tunneling (on a single pre-calculated electronic surface) was presented in Ref. 234.

The total time-dependent wavefunction of the system is expanded in a multiconfigurational product form (12)

$$\Phi(\mathbf{r}, \mathbf{R}; t) = \sum_k \Psi_k(\mathbf{r}, \mathbf{R}) \chi_k(\mathbf{R}; t) \quad (161)$$

where the adiabatic electronic wavefunctions Ψ_k (which are not explicitly time-dependent but depend parametrically on all nuclear coordinates $\mathbf{R}(t)$ at time t) form an orthonormal basis $\langle \Psi_k | \Psi_l \rangle = \delta_{kl}$ for any configuration \mathbf{R} . Furthermore, the normalized but nonorthogonal time-dependent nuclear wavefunction in a specific electronic state k is expanded

$$\chi_k(\mathbf{R}; t) = \sum_I C_k^I(t) g_k^I(\mathbf{R}; \bar{\mathbf{R}}_k^I(t), \bar{\mathbf{P}}_k^I(t), \bar{\gamma}_k^I(t), \alpha_k^I) \quad (162)$$

in terms of a linear combination of multidimensional traveling Gaussians g_k^I . The latter are represented as products of the time-dependent one-dimensional frozen Gaussians as defined in (160) separately for each nuclear degree of freedom.

Based on this overall ansatz the classical (Hamiltonian) equations of motion for the time-dependent variables associated to the nuclei moving on the k th potential energy surface V_k read

$$\begin{aligned} M \dot{\bar{R}}_k &= \bar{P}_k \\ \dot{\bar{P}}_k &= - \left(\frac{\partial V_k}{\partial \bar{R}} \right)_{\bar{R}_k} \\ \dot{\bar{\gamma}}_k &= \frac{\bar{P}_k^2 - 2\alpha_k}{2M} - V_k(\bar{R}_k) \end{aligned} \quad (163)$$

in Heller’s local harmonic approximation;²³⁰ here only the electronic state index k is shown for simplicity and note that the widths α_k do not change. The time-dependent expansion coefficients in (162) evolve according to the following nuclear Schrödinger equation

$$i\dot{\mathbf{C}}_k = (\mathbf{S}_k)^{-1} \left\{ (\mathbf{H}_{kk} - i\dot{\mathbf{S}}_k) \mathbf{C}_k + \sum_{l \neq k} \mathbf{H}_{kl} \mathbf{C}_l \right\} \quad (164)$$

where the various matrices are defined as follows

$$\begin{aligned} (\mathbf{C}_k)^J &= C_k^J \\ (\mathbf{S}_k)^{JI} &= \langle g_k^J | g_k^I \rangle \\ (\dot{\mathbf{S}}_k)^{JI} &= \langle g_k^J | \dot{g}_k^I \rangle \\ (\mathbf{H}_{kl})^{JI} &= \langle g_k^J | H_{kl} | g_l^I \rangle \end{aligned} \quad (165)$$

in terms of the frozen Gaussian basis set (160).

However, a *global* expansion of the kind (161), even using a time- and space-local basis set such as traveling Gaussians (160), is still computationally very demanding for coupled many-dimensional systems. An important ingredient in the FMS/AIMS approach is to “add in” nuclear basis functions “on demand”, i.e. only when they are needed according to some criterion. The latter is the magnitude of the nonadiabatic coupling for each nuclear basis function, which will be one of the parameters that define the accuracy of such calculations. This implies that additional frozen Gaussians are generated (or “spawned off”) as the system evolves from an adiabatic region into a regime of strong mixing of electronic states. The new basis functions are chosen to have maximum overlap with their parents according to the Franck–Condon principle. After having created new basis functions the Schrödinger equation is propagated further in time. Despite these savings, the scaling of AIMS/FMS is formally still exponential in the number of degrees of freedom, see however Ref. 179 for a more detailed discussion.

The electronic structure theory used in conjunction with the nonadiabatic AIMS approach is based on appropriate *ab initio* multireference quantum chemical methods such as for instance CI, CASSCF, or GVB theories. Since such correlated methods are quite demanding concerning computational effort several further approximations have to be invoked. First of all, the basis sets used in applications are typically the smallest ones that are able to describe ground and excited states (double-zeta quality such as, for example, the aug-cc-pVDZ basis), although very diffuse functions such as Rydberg basis functions would be desirable. Furthermore, the Hamiltonian matrix elements (165) are evaluated in the saddle point approximation. In evaluating the nonadiabatic coupling vectors

$$\mathbf{d}_{kl}^I = \langle \Psi_k | \nabla_I | \Psi_l \rangle \quad (166)$$

the dependence of the orbitals (in which the adiabatic wavefunctions $\{\Psi_k\}$ are expanded) on the nuclear coordinates is neglected, i.e. the gradient is taken with respect to wavefunction expansion coefficients only; here the brackets denote integrating over electronic degrees of freedom only.

In summary, what is achieved in the AIMS/FMS approach is to exploit the “local character” of electronic structure calculations both in space and time.

A detailed assessment of FMS in comparison to Tully’s surface hopping and converged quantum dynamics is presented in Ref. 168 for three triatomic model systems using various parameterizations. For most recent applications of the AIMS method we refer, for instance, to Refs. 235 and 236.

5. Achievements, Problems, and Outlook

The field of first principles nonadiabatic molecular dynamics simulations of large systems has certainly received a significant boost in the last decade or so by the practical implementation of numerical methods going beyond the purely theoretical (not to say academic) stage. However, compared to ground state molecular dynamics methods the nonadiabatic extensions are still in their infancy.

Grossly speaking, theoretical treatment of nonadiabatic dynamics can be separated into two main parts, dealing with nonadiabaticity and solving the multi-state electronic structure problem. For both aspects computational methods are in place, that allow one, in principle, to treat nonadiabatic processes at an arbitrarily high level of accuracy. Non–Born–Oppenheimer molecular dynamics simulations of complex systems with many degrees of freedom, however, only become feasible when the simplest and numerically most efficient schemes to treat both nonadiabaticity and electronic structure are used. With regard to nonadiabatic approaches, this means that, in the near future, it will remain all but impossible to use anything beyond mixed quantum-classical methods. As far as electronic structure methods are concerned, we observe that all methods that have been applied to systems consisting of say 50 to 100 atoms are exclusively based on density functional theory if the entire system is treated on an equal footing. In that case, however, the problem of treating excited states within density functional theory is immediately imminent. As it stands right now the number of practical approaches to excited states within density functional is very limited, as the present review has made apparent, but there is a lot of activity and progress in this field. Once there is larger number of density functional-based methods available it is expected that they will greatly extend the range of applicability of nonadiabatic molecular dynamics just like the successes of gradient-corrected ground state density

functional theory made first principles or *ab initio* molecular dynamics successful and thus popular.

If improved accuracy is traded against system size it is certainly possible, today, to use fairly reliable quantum chemical methods beyond the Hartree–Fock or self-consistent field approximation in order to treat excited states. On the other hand this implies either focusing on small systems *per se*, reducing the dimensionality, or treating only part of the system with a sophisticated correlated method. Currently it seems that a commonly used (although less elegant, certainly less faithful and more cumbersome) way along these lines consists in using hybrid ansatzes. Thus, only the part of the system where excitations are localized is treated by “high-level quantum chemistry” whereas the remainder is coupled to it using simpler methods. Such ideas are in widespread use in the field of biomolecular simulations where excitations are typically localized at well-defined chromophores. However, practical hybrids using different system descriptions always have some *ad hoc* flavor or engineering aspects attached to them so that “equal footing approaches” have their own special appeal. In addition, implementing “proper” (in the sense of strictly energy conserving) molecular dynamics schemes that are stable for “long” propagation times (say of the order of several picoseconds) is a nontrivial task.

In conclusion, the main hurdle seems to be the availability of accurate but nevertheless computationally efficient electronic structure methods that allow the efficient evaluation of both gradients and nonadiabatic couplings for excited electronic states. In view of this the field of first principles nonadiabatic molecular dynamics simulations is a rapidly evolving research area with quite some recent successes but a lot of room for future improvements.

References

1. M.P. Allen and D.J. Tildesley, *Computer Simulation of Liquids* (Clarendon Press, Oxford, 1987).
2. G. Ciccotti, D. Frenkel and I.R. McDonald, *Simulation of Liquids and Solids* (North-Holland, Amsterdam, 1987).
3. R. Haberlandt, S. Fritzsche, G. Peinel and K. Heinzinger, *Molekulardynamik — Grundlagen und Anwendungen* (Vieweg Verlag, Braunschweig, 1995).
4. D. Frenkel and B. Smit, *Understanding Molecular Simulation. From Algorithms to Applications* (Academic Press, Boston, 1996).
5. K. Binder and G. Ciccotti (eds.), *Monte Carlo and Molecular Dynamics of Condensed Matter Systems* (Italian Physical Society SIF, Bologna, 1996).
6. B.J. Berne, G. Ciccotti and D.F. Coker, *Classical and Quantum Dynamics in Condensed Phase Simulations* (World Scientific, Singapore, 1998).
7. R. Esser, P. Grassberger, J. Grotendorst and M. Lewerenz (eds.), *Molecular Dynamics on Parallel Computers* (World Scientific, Singapore, 2000).
8. M.E. Tuckerman and G.J. Martyna, *J. Phys. Chem.* **B104**, 159 (2000), see also Addendum: 50 *J. Phys. Chem.* **B105**, 7598 (2001).
9. J. Grotendorst, D. Marx and A. Muramatsu (eds.), *Quantum Simulations of Complex Many-Body Systems: From Theory to Algorithms* (NIC, FZ Jülich, 2002), for downloads see <http://www.fz-juelich.de/nic-series/volume10> and for audio-visual Lecture Notes see <http://www.fz-juelich.de/video/wsqs/>
10. R. Car and M. Parrinello, *Phys. Rev. Lett.* **55**, 2471 (1985).
11. D. Marx and J. Hutter, *Modern Methods and Algorithms of Quantum Chemistry*, ed. J. Grotendorst (NIC, Jülich, 2000), for downloads see <http://www.theochem.ruhr-uni-bochum.de/go/cprev.html>
12. Physics and Astronomy Classification Scheme (PACS); see <http://publish.aps.org/PACS>.
13. D.K. Remler and P.A. Madden, *Mol. Phys.* **70**, 921 (1990).
14. G. Galli and M. Parrinello, *Computer Simulations in Materials Science*, eds. M. Meyer and V. Pontikis (Kluwer, Dordrecht, 1991).
15. M.C. Payne, M.P. Teter, D.C. Allan, T.A. Arias and J.D. Joannopoulos, *Rev. Mod. Phys.* **64**, 1045 (1992).
16. G. Galli and A. Pasquarello, *Computer Simulation in Chemical Physics* (Kluwer, Dordrecht, 1993).
17. E. Deumens, A. Diz, R. Longo and Y. Öhrn, *Rev. Mod. Phys.* **66**, 917 (1994).
18. M.E. Tuckerman, P.J. Ungar, T. von Rosenvinge and M.L. Klein, *J. Phys. Chem.* **100**, 12878 (1996).
19. M.J. Gillan, *Contemp. Phys.* **38**, 115 (1997).
20. M. Parrinello, *Solid State Commun.* **102**, 107 (1997).
21. E. Sandré and A. Pasturel, *Mol. Simul.* **20**, 63 (1997).
22. D. Marx, *Nachr. Chem. Tech. Lab.* **47**, 186 (1999).
23. M.E. Tuckerman, *Quantum Simulations of Complex Many-Body Systems: From Theory to Algorithms*, eds. J. Grotendorst, D. Marx and A. Muramatsu (NIC, FZ Jülich, 2002), for downloads see <http://www.fz-juelich.de/nic-series/volume10/tuckerman2.pdf> and for audio-visual Lecture Notes see <http://www.fz-juelich.de/video/wsqs/>
24. D. Marx and M. Parrinello, *Z. Phys.* **B95**, 143 (1994), a misprinted sign in the Lagrangian is correctly given in Ref. 11.
25. D. Marx and M. Parrinello, *J. Chem. Phys.* **104**, 4077 (1996).

26. M.E. Tuckerman, D. Marx, M.L. Klein and M. Parrinello, *J. Chem. Phys.* **104**, 5579 (1996).
27. D. Marx, M.E. Tuckerman and G.J. Martyna, *Comput. Phys. Commun.* **118**, 166 (1999).
28. M.E. Tuckerman, B.J. Berne, G.J. Martyna and M.L. Klein, **99**, 2796 (1993).
29. M.E. Tuckerman and A. Hughes, *Classical and Quantum Dynamics in Condensed Phase Simulations*, eds. B.J. Berne, G. Ciccotti and D.F. Coker (World Scientific, Singapore, 1998).
30. M.E. Tuckerman, *Quantum Simulations of Complex Many-Body Systems: From Theory to Algorithms*, eds. J. Grotendorst, D. Marx and A. Muramatsu (NIC, FZ Jülich, 2002), for downloads see <http://www.fz-juelich.de/nic-series/volume10/tuckerman1.pdf> and for audio-visual Lecture Notes see <http://www.fz-juelich.de/video/wsqs/>
31. U. Weiss, *Quantum Dissipative Systems* (World Scientific, Singapore, 1999).
32. R.R. Birge, *Biochim. Biophys. Acta* **1016**, 293 (1990).
33. M. Klessinger and J. Michl, *Excited States and Photochemistry of Organic Molecules* (VCH, New York, 1995).
34. A.H. Zewail, *Femtochemistry: Ultrafast Dynamics of the Chemical Bond* (World Scientific, Singapore, 1994).
35. W. Domcke and G. Stock, *Adv. Chem. Phys.* **100**, 1 (1997).
36. D.R. Yarkony, *Rev. Mod. Phys.* **68**, 985 (1996).
37. H. Köppel, W. Domcke and L.S. Cederbaum, *Adv. Chem. Phys.* **57**, 59 (1984).
38. M.A. Robb, M. Garavelli, M. Olivucci and F. Bernardi, *Rev. Comp. Ch.* **15**, 87 (2000).
39. F.O. Ellison, *J. Am. Chem. Soc.* **85**, 3540 (1963).
40. J.C. Tully, *J. Chem. Phys.* **59**, 5122 (1973).
41. J.C. Tully, *J. Chem. Phys.* **58**, 1396 (1973).
42. J.C. Tully, *J. Chem. Phys.* **64**, 3182 (1976).
43. J.C. Tully and C.M. Truesdale, *J. Chem. Phys.* **65**, 1002 (1976).
44. P.J. Kuntz and A.C. Roach, *J. Chem. Soc. Faraday Trans.* **68**, 259 (1971).
45. E. Steiner, P.R. Certain and P.J. Kuntz, *J. Chem. Phys.* **59**, 47 (1973).
46. P.J. Kuntz, *J. Phys.* **B19**, 1731 (1986).
47. A.C. Roach and P.J. Kuntz, *J. Chem. Phys.* **84**, 822 (1986).
48. J.C. Tully, *Modern Theoretical Chemistry*, ed. G.A. Segal (Plenum Press, New York, 1977), Vol. 7A.
49. P.J. Kuntz, *Atom-Molecule Collision Theory*, ed. R.B. Bernstein (Plenum Press, New York, 1979).
50. P.J. Kuntz, *Theory of Chemical Reaction Dynamics*, ed. M. Baer (Chemical Rubber, Boca Raton, 1985), Vol. 1.
51. P.J. Kuntz, *Theoretical Models of Chemical Bonding*, ed. Z.B. Maksic (Springer, Berlin, 1990), Part 2.
52. N.L. Doltsinis and P.J. Knowles, *Chem. Phys. Lett.* **325**, 648 (2000).
53. N.L. Doltsinis, *Mol. Phys.* **97**, 847 (1999).
54. N.L. Doltsinis and P.J. Knowles, *Chem. Phys. Lett.* **301**, 241 (1999).
55. N.L. Doltsinis, P.J. Knowles and F.Y. Naumkin, *Mol. Phys.* **96**, 749 (1999).
56. R. Parson and J. Faeder, *Science* **276**, 1660 (1997).
57. R. Parson, J. Faeder and N. Delaney, *J. Phys. Chem.* **A104**, 9653 (2000).
58. V.S. Batista and D.F. Coker, *J. Chem. Phys.* **106**, 7102 (1997).
59. V.S. Batista and D.F. Coker, *J. Chem. Phys.* **110**, 6583 (1999).
60. S. Goedecker, *Rev. Mod. Phys.* **71**, 1085 (1999).
61. P. Knowles, M. Schütz and H.-J. Werner, *Modern Methods and Algorithms of Quantum Chemistry*, ed. J. Grotendorst (NIC, FZ Jülich, 2000), for downloads see <http://www.fz-juelich.de/nic-series/Volume1/knowles.pdf>
62. M. Schütz, *J. Chem. Phys.* **113**, 9986 (2000).
63. M. Schütz and H.-J. Werner, *J. Chem. Phys.* **114**, 661 (2001).
64. G. Granucci, M. Persico and A. Toniolo, *J. Chem. Phys.* **114**, 10608 (2001).
65. A. Toniolo, M. Ben-Nun and T.J. Martínez, *J. Phys. Chem.* **A106**, 4679 (2002).
66. M. Garavelli, F. Bernardi, M. Olivucci, M.J. Bearpark, S. Klein and M.A. Robb, *J. Phys. Chem.* **A105**, 11496 (2001).
67. M.J. Bearpark, P. Celani, F. Jolibois, M. Olivucci, M.A. Robb and F. Bernardi, *Mol. Phys.* **96**, 645 (1999).
68. F. Eckert and H.J. Werner, *Chem. Phys. Lett.* **302**, 208 (1999).
69. K. Thompson and T.J. Martínez, *J. Chem. Phys.* **110**, 1376 (1999).
70. R.G. Parr and W. Yang, *Density Functional Theory of Atoms and Molecules* (Oxford University Press, Oxford, 1989).
71. R.M. Dreizler and E.K.U. Gross, *Density-Functional Theory* (Springer, Berlin, 1990).
72. P. Hohenberg and W. Kohn, *Phys. Rev.* **B136**, 864 (1964).
73. W. Kohn and L.J. Sham, *Phys. Rev.* **A140**, 1133 (1965).
74. W. Kołos, *Adv. Quant. Chem.* **5**, 99 (1970).
75. W. Kutzelnigg, *Mol. Phys.* **90**, 909 (1997).
76. C.A. Mead, *Rev. Mod. Phys.* **64**, 51 (1992).
77. G. Sutmann, *Quantum Simulations of Complex Many-Body Systems: From Theory to Algorithms*, eds. J. Grotendorst, D. Marx and A. Muramatsu (NIC, FZ Jülich, 2002), for downloads see <http://www.fz-juelich.de/nic-series/volume10/sutmann.pdf> and for audio-visual Lecture Notes see <http://www.fz-juelich.de/video/wsqs/>

78. C. Leforestier, *J. Chem. Phys.* **68**, 4406 (1978).
79. T. Helgaker, E. Uggerud and H.J.A. Jensen, *Chem. Phys. Lett.* **173**, 145 (1990).
80. J.C. Greer, R. Ahlrichs and I.V. Hertel, *Z. Phys.* **D18**, 413 (1991).
81. M.J. Field, *J. Phys. Chem.* **95**, 5104 (1991).
82. E. Uggerud and T. Helgaker, *J. Am. Chem. Soc.* **114**, 4265 (1992).
83. S.A. Maluendes and M. Dupuis, *Int. J. Quant. Chem.* **42**, 1327 (1992).
84. B. Hartke and E.A. Carter, *Chem. Phys. Lett.* **189**, 358 (1992).
85. B. Hartke, D.A. Gibson and E.A. Carter, *Int. J. Quant. Chem.* **45**, 59 (1993).
86. J. Jellinek, V. Bonačić-Koutecký, P. Fantucci and M. Wiechert, *J. Chem. Phys.* **101**, 10092 (1994).
87. A. Heidenreich and J. Sauer, *Z. Phys.* **D35**, 279 (1995).
88. H.-H. Bueker, T. Helgaker, K. Ruud and E. Uggerud, *J. Phys. Chem.* **100**, 15388 (1996).
89. B. Hartke and E.A. Carter, *J. Chem. Phys.* **97**, 6569 (1992).
90. B. Hartke and E.A. Carter, *Chem. Phys. Lett.* **216**, 324 (1993).
91. D.A. Gibson and E.A. Carter, *J. Phys. Chem.* **97**, 13429 (1993).
92. D.A. Gibson, I.V. Ionova and E.A. Carter, *Chem. Phys. Lett.* **240**, 261 (1995).
93. D.A. Gibson and E.A. Carter, *Mol. Phys.* **89**, 1265 (1996).
94. A.J.R. da Silva, M.R. Radeke and E.A. Carter, *Surf. Sci. Lett.* **381**, L628 (1997).
95. A.J.R. da Silva, J.W. Pang, E.A. Carter and D. Neuhauser, *J. Phys. Chem.* **A102**, 881 (1998).
96. Z. Liu, L.E. Carter and E.A. Carter, *J. Phys. Chem.* **99**, 4355 (1995).
97. M. Hartmann, J. Pittner and V. Bonačić-Koutecký, *J. Chem. Phys.* **114**, 2106 (2001).
98. F. Mauri, R. Car and E. Tosatti, *Europhys. Lett.* **24**, 431 (1993), see in particular the discussion revolving around Eq. (8).
99. F. Mauri, *New Developments in Quantum Molecular Dynamics: Excited State Dynamics and Large Scale Simulations*, Ph.D. Thesis (University of Geneva, 1994).
100. R. Car, *Monte Carlo and Molecular Dynamics of Condensed Matter Systems*, eds. K. Binder and G. Ciccotti (Italian Physical Society SIF, Bologna, 1996), see in particular Chap. 23.6.
101. J.K.L. MacDonald, *Phys. Rev.* **46**, 828 (1934).
102. S.M. Valone and J.F. Capitani, *Phys. Rev.* **A23**, 2127 (1981).
103. F. Mauri and R. Car, *Phys. Rev. Lett.* **75**, 3166 (1995).
104. T. Ziegler, A. Rauk and E.J. Baerends, *Theor. Chim. Acta* **43**, 261 (1977).
105. T. Ziegler, *Chem. Rev.* **91**, 651 (1991).
106. U. von Barth, *Phys. Rev.* **A20**, 1693 (1979).
107. B.I. Dunlap, *Chem. Phys.* **125**, 89 (1988).
108. C. Daul, *Int. J. Quant. Chem.* **52**, 867 (1994).
109. A.C. Stückl, C.A. Daul and H.U. Güdel, *Int. J. Quant. Chem.* **61**, 579 (1997).
110. I. Frank, J. Hutter, D. Marx and M. Parrinello, *J. Chem. Phys.* **108**, 4060 (1998).
111. J. Gräfenstein, E. Kraka and D. Cremer, *Chem. Phys. Lett.* **288**, 593 (1998).
112. J. Gräfenstein and D. Cremer, *Phys. Chem. Chem. Phys.* **2**, 2091 (2000).
113. M. Filatov and S. Shaik, *Chem. Phys. Lett.* **288**, 689 (1998).
114. M. Filatov and S. Shaik, *J. Chem. Phys.* **110**, 116 (1999).
115. M. Filatov and S. Shaik, *Chem. Phys. Lett.* **304**, 429 (1999).
116. C. Molteni, I. Frank and M. Parrinello, *J. Am. Chem. Soc.* **121**, 12177 (1999).
117. M. Odellius, D. Laikov and J. Hutter, preprint.
118. N.L. Doltsinis and D. Marx, *Phys. Rev. Lett.* **88**, 166402 (2002).
119. C.C.J. Roothaan, *Rev. Mod. Phys.* **32**, 179 (1960).
120. S. Goedecker and C.J. Umrigar, *Phys. Rev.* **A55**, 1765 (1997).
121. CPMD 3.4: J. Hutter, P. Ballone, M. Bernasconi, P. Focher, E. Fois, S. Goedecker, D. Marx, M. Parrinello and M. Tuckerman, MPI für Festkörperforschung, Stuttgart and IBM Zurich Research Laboratory.
122. J.B. Krieger, Y. Li and G.J. Iafrate, *Phys. Rev.* **A45**, 101 (1992).
123. C.A. Ullrich, U.J. Gossmann and E.K.U. Gross, *Phys. Rev. Lett.* **74**, 872 (1995).
124. E. Runge and E.K.U. Gross, *Phys. Rev. Lett.* **52**, 997 (1984).
125. E.K.U. Gross and W. Kohn, *Adv. Quant. Chem.* **21**, 255 (1990).
126. R. Singh and B.M. Deb, *Phys. Rep.* **311**, 47 (1999).
127. M.E. Casida, *Recent Advances in Density-Functional Methods*, ed. D.P. Chong (World Scientific, Singapore, 1995), p. 155.
128. M. Petersilka, U.J. Grossmann and E.K.U. Gross, *Phys. Rev. Lett.* **76**, 1212 (1996).
129. E.K.U. Gross, J.F. Dobson and M. Petersilka, *Density Functional Theory II*, ed. R.F. Nastajewski (Springer, Heidelberg, 1996), Topics in Current Chemistry.
130. C. Jamorski, M.E. Casida and D.R. Salahub, *J. Chem. Phys.* **104**, 5134 (1996).
131. R. Bauernschmitt and R. Ahlrichs, *Chem. Phys. Lett.* **256**, 454 (1996).
132. D.J. Tozer and N.C. Handy, *J. Chem. Phys.* **109**, 10180 (1998).

133. P.R.T. Schipper, O.V. Gritsenko, S.J.A. van Gisbergen and E.J. Baerends, *J. Chem. Phys.* **112**, 1344 (2000).
134. C. van Caillie and R.D. Amos, *Chem. Phys. Lett.* **308**, 249 (1999).
135. C. van Caillie and R.D. Amos, *Chem. Phys. Lett.* **317**, 159 (2000).
136. J. Hutter, private communication.
137. E.R. Bittner and D.S. Kosov, *J. Chem. Phys.* **110**, 6645 (1999).
138. N.L. Doltsinis and M. Sprik, *Chem. Phys. Lett.* **330**, 563 (2000).
139. E.E. Nikitin, *Chemische Elementarprozesse*, ed. H. Hartmann (Springer, Berlin, 1968).
140. E.E. Nikitin and L. Zülicke, *Theory of Chemical Elementary Processes* (Springer, Berlin, 1978).
141. J.C. Tully and R.K. Preston, *J. Chem. Phys.* **55**, 562 (1971).
142. J.C. Tully, *J. Chem. Phys.* **93**, 1061 (1990).
143. J.C. Tully, *Int. J. Quant. Chem.* **25**, 299 (1991).
144. J.C. Tully, *Classical and Quantum Dynamics in Condensed Phase Simulations*, eds. B.J. Berne, G. Ciccotti and D.F. Coker (World Scientific, Singapore, 1998).
145. J.C. Tully, *Modern Methods for Multidimensional Dynamics Computations in Chemistry*, ed. D.L. Thompson (World Scientific, Singapore, 1998).
146. J.C. Tully, *Faraday Discuss.* **110**, 407 (1998).
147. K. Drukker, *J. Comput. Phys.* **153**, 225 (1999).
148. N.L. Doltsinis, *Quantum Simulations of Complex Many-Body Systems: From Theory to Algorithms*, eds. J. Grotendorst, D. Marx and A. Muramatsu (NIC, FZ Jülich, 2002), for downloads see <http://www.fz-juelich.de/nic-series/volume10/doltsinis.pdf> and for audio-visual Lecture Notes see <http://www.fz-juelich.de/video/wsqs/>
149. L. Salem, *Electrons in Chemical Reactions: First Principles* (Wiley, New York, 1982).
150. L. Salem, C. Leforestier, G. Segal and R. Wetmore, *J. Am. Chem. Soc.* **97**, 479 (1975).
151. H.S.W. Massey, *Rep. Progr. Phys.* **12**, 248 (1949).
152. M. Desouter-Lecomte and J.C. Lorquet, *J. Chem. Phys.* **71**, 4391 (1979).
153. J.C. Tully, M. Gomez and M. Head-Gordon, *J. Vac. Sci. Technol.* **A11** 1914 (1993).
154. S. Klein, M.J. Bearpark, B.R. Smith, M.A. Robb, M. Olivucci and F. Bernardi, *Chem. Phys. Lett.* **292**, 259 (1998).
155. D.F. Coker and L. Xiao, *J. Chem. Phys.* **102**, 496 (1995).
156. U. Muller and G. Stock, *J. Chem. Phys.* **107**, 6230 (1997).
157. S. Hammes-Schiffer and J.C. Tully, *J. Chem. Phys.* **101**, 4657 (1994).
158. S. Hammes-Schiffer and J.C. Tully, *J. Chem. Phys.* **103**, 8528 (1995).
159. F. Webster, P.J. Rossky and R.A. Friesner, *Comput. Phys. Commun.* **63**, 494 (1991).
160. F.J. Webster, J. Schnitker, M.S. Friedrichs, R.A. Friesner and P.J. Rossky, *Phys. Rev. Lett.* **66**, 3172 (1991).
161. E.R. Bittner and P.J. Rossky, *J. Chem. Phys.* **103**, 8130 (1995).
162. E.R. Bittner and P.J. Rossky, *J. Chem. Phys.* **107**, 8611 (1997).
163. M.D. Hack and D.G. Truhlar, *J. Chem. Phys.* **114**, 2894 (2001).
164. M.D. Hack and D.G. Truhlar, *J. Chem. Phys.* **114**, 9305 (2001).
165. Y.L. Volobuev, M.D. Hack, M.S. Topaler and D.G. Truhlar, *J. Chem. Phys.* **112**, 9716 (2000).
166. U. Manthe and H. Köppel, *J. Chem. Phys.* **93**, 1658 (1990).
167. L. Seidner and W. Domcke, *Chem. Phys.* **186**, 27 (1994).
168. M.D. Hack, A.M. Wensmann, D.G. Truhlar, M. Ben-Nun and T.J. Martínez, *J. Chem. Phys.* **115**, 1172 (2001).
169. J. Mavri, *Mol. Simul.* **23**, 389 (2000).
170. T. Kreibich, M. Lein, V. Engel and E.K.U. Gross, *Phys. Rev. Lett.* **87**, 103901 (2001).
171. A.D. McLachlan, *Mol. Phys.* **8**, 39 (1964).
172. P.-G. Reinhard, *Z. Phys.* **A280**, 281 (1977).
173. P. Kramer and M. Saraceno, *Geometry of the Time-Dependent Variational Principle in Quantum Mechanics* (Springer, Berlin, 1981).
174. F. Grossmann, *Comments At. Mol. Phys.* **34**, 141 (1999).
175. E. Deumens and Y. Öhrn, *J. Phys. Chem.* **A105**, 2660 (2001).
176. H. Feldmeier and J. Schnack, *Rev. Mod. Phys.* **72**, 655 (2000).
177. H.-D. Meyer, U. Manthe and L.S. Cederbaum, *Chem. Phys. Lett.* **165**, 73 (1990).
178. M.H. Beck, A. Jäckle, G.A. Worth and H.-D. Meyer, *Phys. Rep.* **324**, 1 (2000), see also <http://www.pci.uni-heidelberg.de/tc/usr/mctdh/>
179. M. Ben-Nun, J. Quenneville and T.J. Martínez, *J. Phys. Chem.* **A104**, 5161 (2000).
180. M. Hartmann, J. Pittner and V. Bonačić-Koutecký, *J. Chem. Phys.* **114**, 2123 (2001).
181. D.G. Truhlar and M.S. Gordon, *Science* **249**, 491 (1990).
182. C. Gonzales and H.B. Schlegel, *J. Phys. Chem.* **94**, 5523 (1990).
183. T. Vreven, F. Bernardi, M. Garavelli, M. Olivucci, M.A. Robb and H.B. Schlegel, *J. Am. Chem. Soc.* **119**, 12687 (1997).
184. A. Selloni, P. Carnevali, R. Car and M. Parrinello, *Phys. Rev. Lett.* **59**, 823 (1987).
185. E.S. Fois, A. Selloni, M. Parrinello and R. Car, *J. Phys. Chem.* **92**, 3268 (1988).

186. E. Fois, A. Selloni and M. Parrinello, *Phys. Rev.* **B39**, 4812 (1989).
187. J. Theilhaber, *Phys. Rev.* **B46**, 12990 (1992).
188. K. Yabana and G.F. Bertsch, *Phys. Rev.* **B54**, 4484 (1996).
189. K. Yabana and G.F. Bertsch, *Int. J. Quant. Chem.* **75**, 55 (1999).
190. U. Saalmann and R. Schmidt, *Z. Phys.* **D38**, 153 (1996).
191. U. Saalmann, *Nicht-adiabatische Quantenmolekulardynamik — Ein neuer Zugang zur Dynamik atomarer Vielteilchensysteme*, Ph.D. Thesis (Technische Universität Dresden, 1997).
192. R. Schmidt, O. Knospe and U. Saalmann, *Il Nuovo Chim.* **A110**, 1201 (1997).
193. U. Saalmann and R. Schmidt, *Phys. Rev. Lett.* **80**, 3213 (1998).
194. O. Knospe, J. Jellinek, U. Saalmann and R. Schmidt, *Eur. Phys. J.* **D5**, 1 (1999).
195. T. Kunert and R. Schmidt, *Phys. Rev. Lett.* **86**, 5258 (2001).
196. T. Kunert and R. Schmidt (2002), preprint.
197. T. Niehaus, *Entwicklung approximativer Methoden in der zeitabhängigen Dichtefunktionaltheorie*, Ph.D. Thesis (Universität Paderborn, 2001).
198. B. Torralva, T.A. Niehaus, M. Elstner, S. Suhai, T. Frauenheim and R.E. Allen, *Phys. Rev.* **B64**, 153105 (2001).
199. W.H. Press, S.A. Teukolsky, W.T. Vetterling and B.P. Flannery, *Numerical Recipes in Fortran 77* (Cambridge University Press, 1999), Vol. 1.
200. A. Alavi, J. Kohanoff, M. Parrinello and D. Frenkel, *Phys. Rev. Lett.* **73**, 2599 (1994).
201. A. Alavi, *Monte Carlo and Molecular Dynamics of Condensed Matter Systems*, eds. K. Binder and G. Ciccotti (Italian Physical Society SIF, Bologna, 1996).
202. N. Marzari, D. Vanderbilt and M.C. Payne, *Phys. Rev. Lett.* **79**, 1337 (1997).
203. J. Cao and B.J. Berne, *J. Chem. Phys.* **99**, 2902 (1993).
204. P.L. Silvestrelli, A. Alavi, M. Parrinello and D. Frenkel, *Phys. Rev. Lett.* **77**, 3149 (1996).
205. P.L. Silvestrelli, A. Alavi, M. Parrinello and D. Frenkel, *Phys. Rev.* **B56**, 3806 (1997).
206. P.L. Silvestrelli and M. Parrinello, *J. Appl. Phys.* **83**, 2478 (1998).
207. A. Gambirasio, M. Bernasconi, G. Benedek and P.L. Silvestrelli, *Phys. Rev.* **B62**, 12644 (2000).
208. A. Alavi, private communication.
209. A. Szabo and N.S. Ostlund, *Modern Quantum Chemistry — Introduction to Advanced Electronic Structure Theory* (McGraw-Hill, New York, 1989).
210. R. McWeeny, *Methods of Molecular Quantum Mechanics* (Academic Press, London, 1992).
211. N.D. Mermin, *Phys. Rev.* **137**, A1441 (1965).
212. C.-L. Fu and K.-M. Ho, *Phys. Rev.* **B28**, 5480 (1983).
213. M.J. Gillan, *J. Phys.: Condens. Matter* **1**, 689 (1989).
214. G.W. Fernando, G.-X. Qian, M. Weinert and J.W. Davenport, *Phys. Rev.* **B40**, 7985 (1989).
215. M. Weinert and J.W. Davenport, *Phys. Rev.* **B45**, 13709 (1992).
216. R.M. Wentzcovitch, J.L. Martins and P.B. Allen, *Phys. Rev.* **B45**, 11372 (1992).
217. G. Kresse and J. Hafner, *Phys. Rev.* **B47**, 558 (1993).
218. M.P. Grumbach, D. Hohl, R.M. Martin and R. Car, *J. Phys.: Condens. Matter* **6**, 1999 (1994).
219. G. Kresse and J. Furthmüller, *Phys. Rev.* **B54**, 11169 (1996).
220. A. Alavi, M. Parrinello and D. Frenkel, *Science* **269**, 1252 (1995).
221. N. Marzari, D. Vanderbilt, A.D. Vita and M.C. Payne, *Phys. Rev. Lett.* **82**, 3296 (1999).
222. N. Marzari and R. Car, *Abstr. Paper Am. Chem. Soc.* **222**, 195 (2001).
223. N. Marzari, private communication.
224. P. Tangney and S. Fahy, *Phys. Rev. Lett.* **82**, 4340 (1999).
225. N.I. Gidopoulos, P.G. Papaconstantinou and E.K.U. Gross, *Phys. Rev. Lett.* **88**, 033003 (2002).
226. T.J. Martínez, M. Ben-Nun and G. Ashkenazi, *J. Chem. Phys.* **104**, 2847 (1996).
227. T.J. Martínez, M. Ben-Nun and R.D. Levine, *J. Phys. Chem.* **100**, 7884 (1996).
228. E.J. Heller, *J. Chem. Phys.* **62**, 1544 (1975).
229. H. Helm, *Phys. Rev.* **A14**, 680 (1976).
230. E.J. Heller, *Acc. Chem. Res.* **14**, 368 (1981).
231. T.J. Martínez and R.D. Levine, *J. Chem. Phys.* **105**, 6334 (1996).
232. T.J. Martínez and R.D. Levine, *Chem. Phys. Lett.* **259**, 252 (1996).
233. T.J. Martínez, *Chem. Phys. Lett.* **272**, 139 (1997).
234. M. Ben-Nun and T.J. Martínez, *J. Chem. Phys.* **112**, 6113 (2000).
235. S. Olsen, L. Manohar and T.J. Martínez, *Biophys. J.* **82**, 1747 (2002).
236. M. Ben-Nun, F. Molnar, K. Schulten and T.J. Martínez, *Proc. Natl. Acad. Sci. USA* **99**, 1769 (2002).